STATISTICS, OPTIMIZATION AND INFORMATION COMPUTING
Stat., Optim. Inf. Comput., Vol. **12**, November 2024, pp 1573–1600.
Published online in International Academic Press (www.IAPress.org)

The Weighted XGamma Model: Estimation, Risk Analysis and Applications

Majid Hashempour [1,*], Morad Alizadeh [2], Haitham M. Yousof [3]

[1]*Department of Statistics, School of Sciences, University of Hormozgan, Bandar Abbas, Iran*
[2]*Department of Statistics, Faculty of Intelligent Systems Engineering and Data Science, Persian Gulf University, Bushehr, 75169, Iran*
[3]*Department of Statistics, Mathematics and Insurance, Benha University, Egypt*

Abstract The weighted XGamma distribution, a new weighted two-parameter lifespan distribution, is introduced in this study. Theoretical characteristics of this model are deduced and thoroughly examined, including quantile function, extreme value, moments, moment generating function, cumulative entropy, and residual cumulative. Some classical estimation methods such as the the maximum likelihood, weighted least square, Anderson Darling and Cramer-von-Mises are considered. A simulation experiments are performed to compare the estimation methods. Four real-life data sets is finally examined to demonstrate the viability of this model. Four key risk indicators are defined and analyzed under the maximum likelihood method. A risk analysis for the exceedances of flood peaks is presented.

Keywords Anderson-Darling; Cullen and Frey plot; Key risk indicators; Risk exposure; Value-at-risk; XGamma model

AMS 2010 subject classifications 62G05; 60E05; 62N05; 62P30.

DOI: 10.19139/soic-2310-5070-1677

1. Introduction

The risk exposure is an actuarial measurement of the possible loss that could occur in the future as a result of a particular action or occurrence. Risks are frequently ranked according to their likelihood of happening in the future multiplied by the potential loss if they did, as part of a study of the business's risk exposure. Ranking the likelihood of probable losses in the future helps the business distinguish between minor and large losses. Speculative risks frequently lead to losses like compliance slip-ups, brand deterioration, security breaches, and liability problems. Due to [41], the risk exposure (RiE$(\cdot)$) can be calculated from

$$\mathrm{RiE}\left(\cdot\right) = \Pr\left(\cdot\right) \times TL\left(\cdot\right), \tag{1}$$

where $\Pr\left(\cdot\right)$ is often derived from historical data, expert judgment, or probabilistic models. It represents the likelihood that a specific event, such as a cyber-attack or natural disaster, will occur, and $TL\left(\cdot\right)$ could be calculated using actuarial methods, historical loss data, or predictive modeling. It reflects the financial or operational impact of the risk event. This framework can be extended to more complex risk environments, incorporating factors such as interdependencies between risks, varying time horizons, and different forms of loss (financial, reputational, etc.). On the other hand, considerable effort has gone into applying time series analysis or continuous distributions to analyse historical insurance data. Recently, several actuaries have used continuous distributions, particularly ones with hefty tails, to represent actual insurance data. In numerous practical fields, including economics, engineering, risk management, dependability, and actuarial sciences, real data has been modelled using continuous heavy-tailed

*Correspondence to: Majid Hashempour (Email: ma.hashempour@hormozgan.ac.ir). Department of Statistics, School of Sciences, University of Hormozgan, Bandar Abbas, Iran.

ISSN 2310-5070 (online) ISSN 2311-004X (print)

probability distributions. The skewedness of the insurance data sets can be left-skewed, right-skewed with hefty tails, or unimodal right-skewed.

Probability-based distributions provide a sufficient framework for describing risk exposure. Often, this risk exposure is summarized using a single figure or, in some cases, a small set of figures that represent the level of risk. These figures, known as key risk indicators (KRIs), are derived from specific statistical models and serve as crucial metrics for assessing risk. Prominent examples of work on KRIs include the studies by [7]. KRIs are essential tools for quantifying the risk associated with various activities. They are used by organizations to provide early warnings about rising risk exposures across different areas of the business. Unlike key performance indicators, which focus on measuring how effectively something is being done, KRIs are concerned with signaling the potential for future negative impacts. They help identify emerging risks that could disrupt the continuity of an activity or project. By monitoring KRIs, organizations can proactively recognize and address potential threats before they escalate into significant issues. This early detection allows for timely interventions that can mitigate risks, thereby protecting the organization from adverse outcomes and ensuring the stability and success of ongoing operations.

The KRIs play a crucial role in providing actuaries and risk managers with valuable insights into a company's exposure to various types of risk. These indicators help quantify the level of risk by focusing on specific metrics that reflect the potential for financial losses or other adverse outcomes. Among the most commonly analyzed KRIs are value-at-risk (VAR), tail-value-at-risk (TVAR), also known as conditional tail expectation (CTE), conditional-value-at-risk (CVAR), tail variance (TV), and tail mean-variance (TMV). Each of these KRIs serves a distinct purpose in risk management (see [7]). For instance, the VAR indicator is particularly significant as it focuses on the quantiles of the distribution of aggregate losses. VAR estimates the maximum potential loss that could occur within a specified confidence level over a given period. This makes it a key tool for determining the amount of capital that should be reserved to cover potential losses in adverse scenarios. By assessing the likelihood and impact of these negative outcomes, VAR enables companies to better prepare for financial uncertainties. The TVAR and the CVAR extend the analysis beyond VAR by focusing on the tail end of the loss distribution, which represents extreme losses that could occur but are less likely. These indicators provide a more comprehensive understanding of risk by considering not just the threshold of loss but also the severity of losses beyond that threshold. The TV and TMV further enrich this analysis by incorporating the variability and mean-variance characteristics of the tail distribution, offering deeper insights into the potential for extreme outcomes. To enhance the accuracy and flexibility of risk assessment, a new statistical model known as the WXGa distribution is introduced in this paper. The weighted XGamma (WXGa) model is designed to provide a better fit for real-life data, especially when analyzing the tail behavior of distributions, which is critical for accurately estimating these KRIs. By applying the WXGa model, actuaries and risk managers can gain a more nuanced understanding of risk exposure, leading to more informed decision-making and improved risk management strategies. This paper explores the properties of the WXGa distribution and demonstrates its effectiveness in modeling risk by applying it to real-life data sets. The results suggest that the WXGa model offers a superior alternative to existing models, particularly when it comes to accurately estimating KRIs and preparing for potential financial risks.

In the manufacturing sector, it is a standard procedure for finished products to undergo a thorough screening inspection before they are dispatched to customers. During this inspection, each product is evaluated to determine whether it meets predefined performance standards, which are typically defined by specific tolerance limits. On the other hand, if a product does not conform to these standards, meaning it falls outside the specified tolerance limits, it is usually not accepted for delivery. Instead, the product is either rejected and discarded as scrap, or it is sent back for rework in an attempt to bring it up to the required standards. This quality control process is crucial for ensuring that only products that meet the specified criteria reach the customers, thereby maintaining the integrity and reliability of the manufacturing process. In this case, the actual distribution to the customer is truncated. For such purposes, the tracated version are presented. However, when specifying the likelihood of events as they are observed and noted, weighted distributions naturally develop by adjusting the likelihood that events will really occur while taking into account the techniques of ascertainment. Making these tweaks could prevent incorrect conclusions from developing.

Recently, [29] explore the Burr type-X Pareto distribution, focusing on its properties and applications in finance. They provide insights into estimating the VAR using this distribution. The study highlights its utility in risk management. [45] introduce the odd log-logistic Weibull family, applying it to regression and financial risk models. Their work addresses the need for flexible models in risk assessment and prediction. [23] present a new compound Lomax model, emphasizing its properties and use in risk analysis with negatively skewed insurance claims data. The study explores copulas and modeling techniques for improved risk assessment. [50] develop an asymmetric density model for risk claim-size data, focusing on prediction and applications with bimodal data. Their work addresses challenges in modeling complex risk data. [1] propose a novel G family of distributions for single acceptance sampling plans, highlighting its applications in quality control and risk decisions. The study offers a new approach to sampling and risk management. [60] introduce a new reciprocal Weibull extension for modeling extreme values, with a focus on risk analysis in insurance data. Their model improves extreme value modeling and risk estimation. [25] compare Bayesian and non-Bayesian methods for risk analysis under left-skewed insurance data. They introduce a compound reciprocal Rayleigh extension, enhancing risk assessment techniques. [61] analyze the bimodal heavy-tailed Burr XII model for insurance data, exploring various methods for risk estimation and analysis. Their work provides a comprehensive approach to modeling heavy-tailed risks. [63] propose a novel model for quantitative risk assessment using bimodal and symmetric data. The study focuses on improving risk modeling and assessment under diverse claim-size data. [27] develop a new family of compound probability distributions, examining their properties, copulas, and applications in reinsurance revenue data. Their work contributes to advanced risk analysis techniques. [62] present a discrete claims-model for inflated and over-dispersed automobile claims frequencies. Their study emphasizes applications and actuarial risk analysis for improved claims management. [33] introduce the quasi-XGamma frailty model, addressing heterogeneity and risk analysis for emergency care data. They focus on survival analysis and validation testing in their model. [53] propose a Two-Parameters Lindley-Frailty Model, assessing both censored and uncensored data schemes. Their work includes applications and validation testing for different baseline models, they also presented some results for risk analysis. [13] develop a new probability model for losses and revenues, incorporating entropy analysis. Their study applies the model to value-at-risk and mean of order-P (MOOP) analyses, enhancing risk modeling techniques. [22] present a new Lindley extension for bimodal right-skewed precipitation data, focusing on estimation and risk assessment. Their model addresses challenges in precipitation data analysis. [3] propose a novel XGamma extension, applying it to reinsurance data for actuarial risk analysis. The study offers a new perspective on risk modeling in the insurance industry. [47] introduce a new Lomax extension, focusing on properties and risk analysis under left-skewed insurance and medical data. Their work includes comprehensive goodness-of-fit validation. [24] develop a right-skewed one-parameter distribution, emphasizing its mathematical characterization and validation. The study applies the distribution to actuarial risk analysis and practical applications. [2] explore the extended Gompertz model, focusing on applications, mean of order P assessment, and statistical threshold risk analysis. Their work is based on extreme stresses data and enhances reliability assessment methods. Finally, [44] presented a new XGamma model using the odd log-logistic G family with Bayesian and some classical estimation methods with risk analysis and assessment under the financial reinsurance revenues data.

Weighted distributions are widely used across various disciplines, such as medicine, ecology, and reliability engineering, to develop more accurate and relevant statistical models. These models are particularly valuable when traditional, or standard, distributions fail to adequately describe the data at hand. In such cases, weighted distributions offer a more flexible approach, allowing for better data modeling and more precise predictions. The utility of weighted distributions lies in their ability to modify standard distributions in a way that accounts for the specific characteristics of the data or the underlying processes being studied. For example, in medicine, weighted distributions might be used to adjust for patient characteristics that affect health outcomes, while in ecology, they might be used to account for sampling biases in wildlife studies. In reliability engineering, these distributions can model the life expectancy of components under different stress conditions. The importance of weighted distributions has led to extensive research in the statistical literature. Numerous studies have been conducted to explore the properties, applications, and advantages of these distributions across different fields. These studies have provided a foundation for the continued development of more sophisticated models that can address a wide range of real-life challenges. One of the more recent contributions to this area of research is the introduction of

the XGamma (XGa) distribution by [49]. The XGa distribution is a novel statistical model that has been designed to provide a better fit for certain types of data where standard distributions might not be adequate. The flexibility of the XGa distribution makes it particularly useful for modeling data with complex characteristics, such as those involving heavy tails or skewness. The cumulative distribution function (CDF) and the probability density function (PDF) of the standard XGa distribution are fundamental to understanding its behavior and applications. The CDF provides the probability that a random variable drawn from the XGa distribution will take on a value less than or equal to a certain threshold, while the PDF describes the likelihood of the random variable taking on specific values within the distribution. These functions form the mathematical foundation of the XGa distribution and are crucial for applying it to data modeling and statistical analysis. By utilizing the XGa distribution, researchers and practitioners in various fields can enhance their ability to model complex data, leading to more accurate predictions and better decision-making. The introduction of the XGa distribution is a significant advancement in the field of weighted distributions, offering new opportunities for statistical modeling and analysis in a variety of applications. The CDF and the PDF of the standard XGa are given by

$$G_\delta(w) = 1 - \left(1 + \frac{\delta\, w}{1+\delta} + \frac{0.5\,\delta^2\, w^2}{1+\delta}\right) e^{-\delta\, w}, \quad g_\delta(w) = \frac{\delta^2}{1+\delta}\,(1 + 0.5\,\delta\, w^2) e^{-\delta\, w}, \tag{2}$$

where $w > 0$ and $\delta > 0$ is the shape parameter. The XGamma distribution is applied successfully to time-to-event data set and its different properties are studied. Building on the work of [49], [**?**] introduced the Exponentiated XGamma (Exp-XGa) distribution. [48] further expanded the XGamma model by developing a compound model known as the quasi XGamma-Poisson distribution. [11] explored a new family of distributions based on Sen et al.'s XGamma model, referred to as the XGamma G family. Additionally, [57] provided statistical validation for the XGamma exponential model by applying the Nikulin-Rao-Robson goodness-of-fit test to both complete and censored samples, using various estimation methods. For further insights, [8] discussed the half-logistic XGamma distribution, [43] examined the Poisson XGamma distribution, and [55] introduced the inverse XGamma distribution. The CDF of the WXGa is given by

$$\Phi_{\delta,\zeta}(w) = \frac{1 - \left[1 + \frac{\delta\, w}{1+\delta} + \Delta_\delta\,(w)\right] e^{-\delta\, w}}{1 + \left[1 + \frac{\zeta\, W}{1+\zeta} + \Delta_\zeta\,(w)\right] e^{-\delta\, w}} \tag{3}$$

where

$$\Delta_\varsigma\,(w) = \frac{0.5}{1+\varsigma}\varsigma^2\, w^2,$$

$w > 0$, $\delta > 0$ and $\zeta > 0$ are two shape parameters. The CDF in (3) is derived by compoundig two XGa random varaibles (RVs). We denote it by $W \sim$WXGa(δ, ζ). The PDF and HRF are given by

$$\begin{aligned}
\phi_{\delta,\zeta}(w) &= \left[\frac{\delta^2}{1+\delta}\left(1 + 0.5\,\delta\, w^2\right)\right] e^{-\delta\, w}\left[1 + \left(1 + \frac{\zeta\, w}{1+\zeta} + \Delta_\zeta\,(w)\right) e^{-\zeta\, w}\right] \\
&+ \frac{\zeta^2}{1+\zeta}(1 + 0.5\,\zeta\, w^2) e^{-\zeta\, w}\left[1 - \left(1 + \frac{\delta\, w}{1+\delta} + \Delta_\delta\,(w)\right) e^{-\delta\, w}\right] \\
&\times \left[1 + \left(1 + \frac{\zeta\, w}{1+\zeta} + \Delta_\zeta\,(w)\right) e^{-\zeta\, w}\right]^{-2},
\end{aligned} \tag{4}$$

and

$$\eta(w;\delta,\zeta) = \frac{\delta^2}{1+\delta}(1+0.5\,\delta\,w^2)e^{-\delta\,w}\left[1+\left(1+\frac{\zeta\,w}{1+\zeta}+\Delta_\zeta\,(w)\right)e^{-\zeta\,w}\right]$$
$$+\frac{\zeta^2}{1+\zeta}(1+0.5\,\zeta\,w^2)e^{-\zeta\,w}\left[1-\left(1+\frac{\delta\,w}{1+\delta}+\Delta_\delta\,(w)\right)e^{-\delta\,w}\right]$$
$$\times\left[1+\left(1+\frac{\zeta\,w}{1+\zeta}+\Delta_\zeta\,(w)\right)e^{-\zeta\,w}\right]$$
$$\times\left\{\left(1+\frac{\delta\,w}{1+\delta}+\Delta_\delta\,(w)\right)e^{-\delta\,w}+\left(1+\frac{\zeta\,w}{1+\zeta}+\Delta_\zeta\,(w)\right)e^{-\zeta\,w}\right\}. \tag{5}$$

Figure 1 gives some plots of new PDF for some value of parameters. Figure 2 provides some plots of new HRF for some value of parameters. Based on Figure 1, The density of the WXGa model can be right-skewed with one peak, bimodal, right-skewed without a peak, left-skewed and unimodal PDF with different shapes. Due to Figure 2, the WXGa model's HRF has several possible shapes, including monotonically increasing, upside-down, bathtub-monotonically increasing, bathtub-bathtub, upside-down-increasing and reversed-J shape (monotonically decreasing). This wide diversity of the novel PDF and its corresponding HRF gives a great advantage in statistical modeling processes and practical applications in various fields. This is because the modeling processes and their related preference for a model over a model is mainly related to the extent of the flexibity of the distribution.

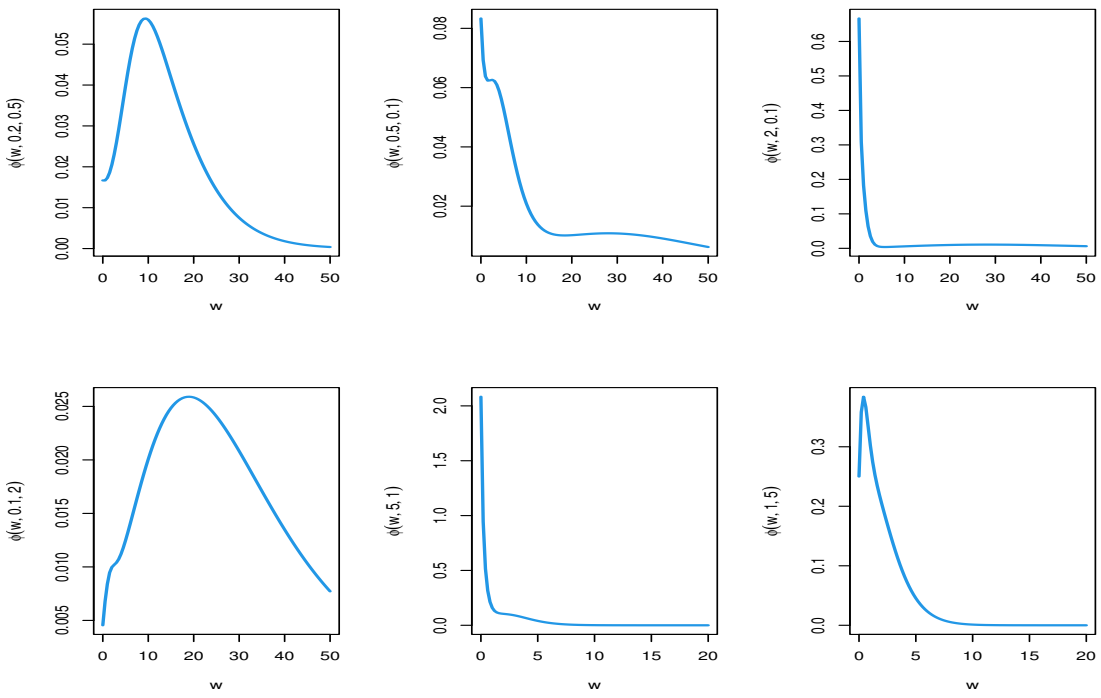

Figure 1. Plots of PDF for some value of parameters.

The following factors motivate us to do this work:

- The WXGa density can be right-skewed, left-skewed, bimodal, and unimodal, as well as right-skewed without a peak. (see Figure 1)**.** The aforementioned traits provide the new distribution with a significant advantage in statistical modelling.

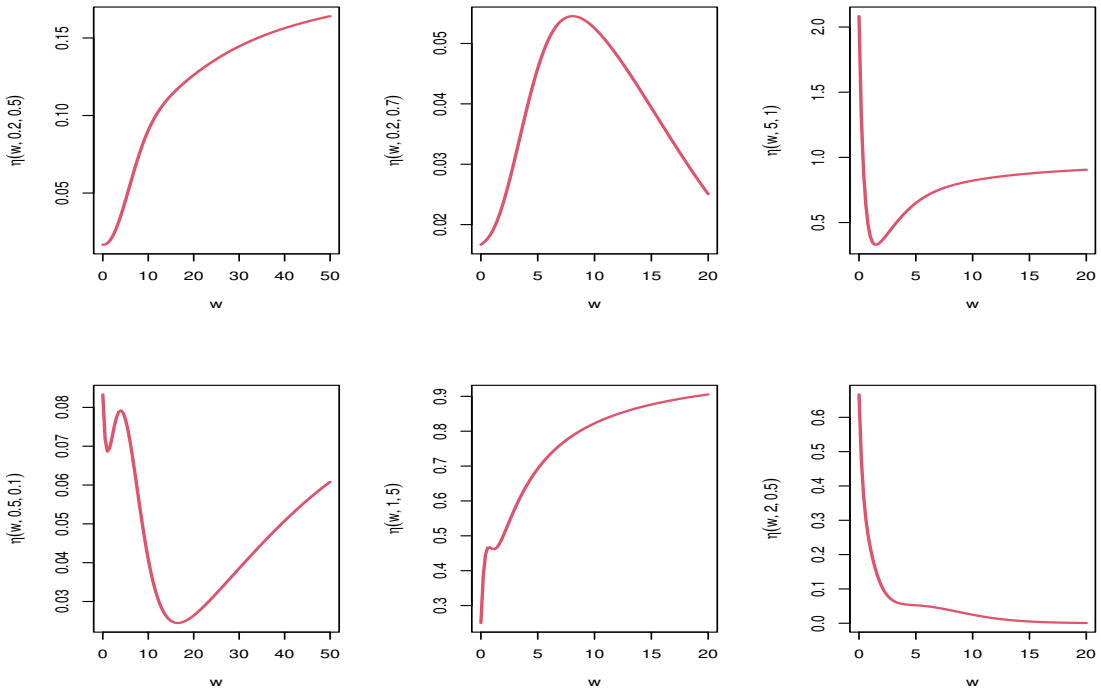

Figure 2. Plots of HRF for some value of parameters.

- The WXGa model's HRF has several possible shapes, including bathtub-bathtub, bathtub-monotonically increasing, reversed-J, upside-down, monotonically increasing, and monotonically decreasing (see Figure 2). We can apply the new model to analyze a wide range of data sets thanks to the HRF's adaptability.
- The WXGa model may be selected as the optimal distribution in the insurance and risk management industries, particularly when modelling left skewness insurance real data.
- Since the WXGa model's density allows for a variety of useful forms, including the left-skewed shape, it has demonstrated its superiority in characterising the left-skewed insurance claims data.
- In field of modeling "upside-down-bathtub", "bathtub", "bathtub" and "upside-down-bathtub" HRF data stes, the WXGa model in recommended.
- In the case of dealing with real data sets which have some extreme observations, the WXGa model provided adequate results.
- For modeling the right skewed asymmetric bimodal it is better to consider a model which exhibits and include the same shape. By comparing Figure 1 and Figure 2, we find that the new model is a strong candidate for modeling this type of data.

The structure of the remainder of this paper is as follows: Section 2 explores various properties of the proposed distribution. Section 3 presents the KRIs under the WXGa model. In Section 4, several classical estimation methods are discussed, including maximum likelihood, weighted least squares, Anderson-Darling, and Cramer-von-Mises. Section 5 features simulation experiments designed to compare these estimation methods. In Section 6, real data sets are analyzed to demonstrate the performance of the new distribution family. Section 7 offers a risk analysis and an application of the model. Finally, Section 8 provides concluding remarks.

2. Main properties

In this part, we study some structural properties of the $W \sim$WXGa(δ, ζ). distribution.

2.1. Quantile function and asymptotics

For $\delta = \zeta$, let $X \sim$Exp(δ) and $Z \sim$Ga$(3, \delta)$, if $\frac{2u}{1+u} \leq \frac{\delta}{1+\delta}$, then $W = X$, otherwise $W = Z$.

For $\delta \neq \zeta$, let $V \sim U(0, 1)$, then the root of equation

$$\frac{1 - \left(1 + \frac{\delta\, w}{1+\delta} + \Delta_\delta\left(w\right)\right) e^{-\delta\, w}}{1 + \left(1 + \frac{\zeta\, x}{1+\zeta} + \Delta_\zeta\left(w\right)\right) e^{-\zeta\, w}} = v \tag{6}$$

has CDF (3). The asymptotic of CDF, PDF and HRF as $w \to 0^+$ are given by

$$\Phi(w) \sim \frac{\delta\, w}{2}, \phi(w) \sim \frac{\delta}{2}\,, \eta(w) \sim \frac{\delta}{2 - \delta\, w}. \tag{7}$$

Let $c = \min\{\delta, \zeta\}$, the asymptotic of CDF, PDF and HRF as$w \to \infty$ are given by

$$1 - \Phi(w) \sim \frac{0.5\, c^2\, w^2}{1 + c}\, \exp\left\{-c\, w\right\}, \phi(w) \sim \frac{0.5\, c^3\, w^2}{1 + c}\, \exp\left\{-c\, w\right\}, \eta(w) \sim c. \tag{8}$$

These equations show the effect of parameters on tails of WXGa distribution.

2.2. Moments

Let $\mu_n = E(W^n)$ denote the n-th moment of W. Now we prove that all moments are exist.

Theorem 1

Let $W \sim WXGa(\delta, \gamma)$, then $E(W^n) < \infty$.

Proof:

$$\begin{aligned}
E(W^n) &= n \int_0^\infty w^{n-1} \left[1 - \Phi(w)\right] dw \\
&= n \int_0^\infty w^{n-1} \frac{(1 + \frac{\gamma\, w}{1+\gamma} + \frac{0.5\, \gamma^2\, w^2}{1+\gamma})\mathrm{e}^{-\gamma\, \mathrm{w}} + (1 + \frac{\delta\, \mathrm{w}}{1+\mathrm{a}} + \frac{0.5\, \delta^2\, \mathrm{w}^2}{1+\delta})\mathrm{e}^{-\delta\, \mathrm{w}}}{1 + (1 + \frac{\gamma\, w}{1+\gamma} + \frac{0.5\, \gamma^2\, w^2}{1+\gamma})\mathrm{e}^{-\gamma\, \mathrm{w}}} dw \\
&< n \int_0^\infty w^{n-1} \left[(1 + \frac{\gamma\, w}{1+\gamma} + \frac{0.5\, \gamma^2\, w^2}{1+\gamma})\mathrm{e}^{-\gamma\, \mathrm{w}} + (1 + \frac{\delta\, \mathrm{w}}{1+\delta} + \frac{0.5\, \delta^2\, \mathrm{w}^2}{1+\delta})\mathrm{e}^{-\delta\, \mathrm{w}}\right] dw < \infty
\end{aligned}$$

We define and compute

$$A(a_1, l, a_2; \zeta) = \int_0^\infty w^{a_1 - 1} \left(1 + \frac{\zeta\, w}{1+\zeta} + \Delta_\zeta\left(w\right)\right)^l e^{-a_2\, w} dw$$

for any $a_1, a_2 > 0$ and $l \in N$. After using multinomial exapansion we can easily obtain

$$A(a_1, l, a_2; \zeta) = \sum_{j_1, j_2 \in A} \frac{l!}{j_1! j_2! (l - j_1! - j_2!)} \left(\frac{\zeta}{1+\zeta}\right)^{j_1} \left(\frac{0.5\, \zeta^2}{1+\zeta}\right)^{j_2} \times \frac{\Gamma(a_1 + j_1 + j_2)}{a_2^{a_1 + j_1 + j_2}}$$

where

$$A = \{(j_1, j_2) | 0 \leq j_1 \leq l, 0 \leq j_2 \leq l, 0 \leq j_1 + j_2 \leq l\}$$

Then we can obtain

$$\begin{aligned}
& E(W^n) = n\int_0^\infty w^{n-1}\left[1-\Phi(w)\right]dw \\
= \; & n\int_0^\infty w^{n-1}\left[\left(1+\frac{\zeta\, w}{1+\zeta}+\Delta_\zeta\left(w\right)\right)e^{-\zeta\, w}+\left(1+\frac{\delta\, w}{1+a}+\Delta_\delta\left(w\right)\right)e^{-\delta\, w}\right]dw \\
& +n\sum_{i=1}^{\infty}(-1)^i\int_0^\infty w^{n-1}(1+\frac{\zeta\, w}{1+\zeta}+\Delta_\zeta\left(w\right))^{i+1}e^{-\zeta(i+1)\, w}dw \\
& +n\sum_{i=1}^{\infty}(-1)^i\int_0^\infty w^{n-1}\left(1+\frac{\zeta\, w}{1+\zeta}+\Delta_\zeta\left(w\right)\right)^{i}\left(1+\frac{\delta\, w}{1+\delta}+\Delta_\delta\left(w\right)\right)e^{-(\delta+\zeta\, i)\, w}dw \\
= \; & \frac{n\,\Gamma(n)}{\zeta^n}+\frac{n\,\Gamma(n+1)}{(1+\zeta)\zeta^n}+\frac{0.5\,n\,\Gamma(n+2)}{(1+\zeta)\zeta^n}+\frac{n\,\Gamma(n)}{\delta^n}+\frac{n\,\Gamma(n+1)}{(1+\delta)\delta^n}+\frac{0.5\,n\,\Gamma(n+2)}{(1+\delta)\delta^n} \\
& +n\sum_{i=1}^{\infty}(-1)^i\,A(n,i+1,\zeta(i+1);\zeta)+n\sum_{i=1}^{\infty}(-1)^i\,A(n,i,\delta+\zeta\, i;\zeta) \\
& +n\,\delta\sum_{i=1}^{\infty}\frac{(-1)^i\,A(n+1,i,\delta+\zeta\, i;\zeta)}{1+\delta}+0.5\,n\,\delta^2\sum_{i=1}^{\infty}\frac{(-1)^i\,A(n+2,i,\delta+\zeta\, i;\zeta)}{1+\delta}
\end{aligned} \tag{9}$$

Based on theorem 1, these series equations are convergent.

2.3. Extreme Value

If $\bar{W}=\frac{W_1+...+W_n}{n}$ denote the sample mean, then using the central limit theorem, $\frac{\sqrt{n}(\bar{W}-E(W))}{\sqrt{\text{Var}(W)}}$ approaches the standard normal distribution as $n\to\infty$. Define extreme values $M_{n,W}=\max(W_1,...,W_n)$ and $m_{n,W}=\min(W_1,...,W_n)$. Let $\tau(z)=\frac{1}{\min\{\delta,\zeta\}}$, we obtain following equations

$$\lim_{t\to 0}\frac{\Phi(t\, w)}{\Phi(t)}=w,\;\lim_{t\to\infty}\frac{1-\Phi(t+w\,\tau(t))}{1-\Phi(t)}=\mathrm{e}^{-w}.$$

Thus, using Theorem 1.6.2 in [32] , there must be norming constants $a_n>0,\quad b_n,\quad c_n>0$ and d_n such that

$$Pr\left[a_{n,W}(M_{n,W}-b_{n,W})\le w\right]\to e^{-e^{-w}},\;\Pr\left[c_{n,W}(m_{n,W}-d_{n,W})\le W\right]\to 1-e^{-w},$$

as $n\to\infty$. The form of the norming constants can also be determined.

2.4. Entropy

Cumulative entropy and cumulative residual entropy (CRE) are most important measure of information. The cumulative entropy and cumulative residual entropy of W are defined by

$$\mathcal{CE}(W)=-\int_0^\infty\Phi(w)\log\left[\Phi(w)\right]dw,\;\mathcal{CRE}(W)=-\int_0^\infty\bar{\Phi}(w)\log\left[\bar{\Phi}(w)\right]dw.$$

First note that

$$\begin{aligned}
& -\Phi(w)\log(\Phi(w))=\frac{1-\left(1+\frac{\delta\, w}{1+\delta}+\Delta_\delta\left(w\right)\right)e^{-\delta\, w}}{1+\left(1+\frac{\zeta\, w}{1+\zeta}+\Delta_\zeta\left(w\right)\right)e^{-\zeta\, w}} \\
& \times\left\{\log\left[1+\left(1+\frac{\zeta\, w}{1+\zeta}+\Delta_\zeta\left(w\right)\right)e^{-\zeta\, w}\right]-\log\left[1-\left(1+\frac{\delta\, w}{1+\delta}+\Delta_\delta\left(w\right)\right)e^{-\delta\, w}\right]\right\}.
\end{aligned}$$

Now we define and compute

$$C(d_1,d_2,d_3;\delta,\zeta)=\int_0^\infty \left(1+\frac{\delta\, w}{1+\delta}+\Delta_\delta\,(w)\right)^{d_1}\left(1+\frac{\zeta\, w}{1+\zeta}+\Delta_\zeta\,(w)\right)^{d_2} e^{-d_3\, z} z$$

Using multinomial exapnsion it is easy to show that

$$C(d_1,d_2,d_3;\delta,\zeta)=\sum_{i_1,i_2\in A}\sum_{j_1,j_2\in B}\frac{v_{i_1,i_2,j_1,j_2}}{d_3^{i_1+j_1+2(i_2+j_2)+1}}\Gamma(i_1+j_1+2(i_2+j_2)+1).$$

where

$$A=\{(i_1,i_2)|0\le i_1\le d_1, 0\le i_2\le d_1, 0\le i_1+i_2\le d_1\},$$
$$B=\{(j_1,j_2)|0\le j_1\le d_2, 0\le j_2\le d_2, 0\le j_1+j_2\le d_2\},$$

$$v_{i_1,i_2,j_1,j_2}=\frac{0.5^{i_2+j_2}\,\delta^{i_1+2\,i_2}\,\zeta^{j_1+2\,j_2}\,d_1!d_2!}{i_1!i_2!(d_1-i_1-i_2)!j_1!j_2!(d_2-j_1-j_2)!(1+\delta)^{i_1+i_2}(1+\zeta)^{j_1+j_2}} \tag{10}$$

then we can obtain

$$\begin{aligned}\mathcal{CE}(W)&=\sum_{k,l=0}^{\infty}\frac{(-1)^l}{k+1}C(k+1,l,\delta(k+1)+\zeta\, l;\delta,\zeta)\\&-\sum_{k,l=0}^{\infty}\frac{(-1)^l}{k+1}C(k+2,l,\delta(k+1)+\zeta\, l;\delta,\zeta),\end{aligned} \tag{11}$$

Also after some simple algebraic calculation we can obtain

$$\begin{aligned}-\bar\Phi(w)\log(\bar\Phi(w))&=-\frac{\left(1+\frac{\delta\, w}{1+\delta}+\Delta_\delta\,(w)\right)e^{-\delta\, w}+\left(1+\frac{\zeta\, w}{1+\zeta}+\Delta_\zeta\,(w)\right)e^{-\zeta\, w}}{1+\left(1+\frac{\zeta\, w}{1+\zeta}+\Delta_\zeta\,(w)\right)e^{-\zeta\, w}}\\&\times\log\left[1-\frac{1-(1+\frac{\delta\, w}{1+\delta}+\Delta_\delta\,(w))e^{-\delta\, w}}{1+(1+\frac{\zeta\, w}{1+\zeta}+\Delta_\zeta\,(w))e^{-\zeta\, w}}\right]\\&=\left[\left(1+\frac{\delta\, w}{1+\delta}+\Delta_\delta\,(w)\right)e^{-\delta\, w}+\left(1+\frac{\zeta\, w}{1+\zeta}+\Delta_\zeta\,(w)\right)e^{-\zeta\, w}\right]\\&\times\sum_{i=0}^{\infty}\frac{1}{i+1}\frac{\left[1-\left(1+\frac{\delta\, w}{1+\delta}+\Delta_\delta\,(w)\right)e^{-\delta\, w}\right]^{i+1}}{\left[1+\left(1+\frac{\zeta\, w}{1+\zeta}+\Delta_\zeta\,(w)\right)e^{-\zeta\, w}\right]^{i+2}}\end{aligned} \tag{12}$$

Now using generalized binomial expansion we can obtain

$$\begin{aligned}-\bar\Phi(w)\log(\bar\Phi(w))&=\left[(1+\frac{\delta\, w}{1+\delta}+\Delta_\delta\,(w))e^{-\delta\, w}+\left(1+\frac{\zeta\, w}{1+\zeta}+\Delta_\zeta\,(w)\right)e^{-\zeta\, w}\right]\\&\times\sum_{i,j=0}^{\infty}\sum_{l=0}^{i+1}q_{i,j,l}\ \left(1+\frac{\delta\, w}{1+\delta}+\Delta_\delta\,(w)\right)^{l}\left(1+\frac{\zeta\, w}{1+\zeta}+\Delta_\zeta\,(w)\right)^{j}e^{-w(\delta\, l+\zeta\, j)}\end{aligned}$$

where

$$q_{i,j,l}=\frac{(-1)^l}{i+1}\binom{-i-2}{j}\binom{i+1}{l}.$$

Finally we can obtain

$$\mathcal{CRE}(W) = \sum_{i,j=0}^{\infty} \sum_{l=0}^{i+1} q_{i,j,l} \left[C(l+1, j, \delta(l+1) + \zeta\, j; \delta, \zeta) - C(l, j+1, \delta\, l + \zeta(j+1); \delta, \zeta) \right].$$

3. KRIs

Evaluating the exposure to market risk in a portfolio of instruments that results from changes in the underlying variables, such as equity prices, interest rates, or currency rates, is one of the most crucial duties of the actuarial sciences institutes. In this part, we compute some KRIs for the proposed distribution, including VAR, TVAR, TV and TMV. These indicators are vital for maximizing a portfolio in the face of uncertainty.

3.1. VAR indicator

The VAR is frequently utilised by practitioners as a standard financial market risk in the context of actuarial sciences. It is sometimes referred to as the quantile premium principle or the quantile risk measure.

Definition 1: *Let W denote a loss random variable (LRV). The VAR of W* at the $100q\%$ *level, say VaRq(W) or $\pi\,(q)$, is the $100q\%$ quantile (or percentile (Q_W)) of the distribution of W.*

Then, based on Definition 1 for the WXGa distribution, we can simply write

$$\Pr\left(W > Q_W\right) = \begin{cases} 1\%|_{q=99\%} \\ 5\%|_{q=95\%} \\ \vdots \end{cases}, \tag{13}$$

where Q_W represents the numerical suotion of (6). From (13), for a one-year time when $q = 99\%$, the interpretation is that there is only a very small chance (1%) that the insurance company will be bankrupted by an adverse outcome over the next year. The quantity VAR$(W; q)$ does not satisfy one of the four criteria for coherence (see [54]).

3.2. TVAR risk indicator

Definition 2: *Let W* denote a *LRV. The TVaRq* of *W at the $100q\%$ confidence level is the expected loss given that the loss exceeds the $100q\%$ of the distribution of W* , namely

$$\text{TVaRq}(W) = \mathbb{E}\left(W | W > \pi\left(q\right)\right) = \frac{1}{1 - \Phi_{\delta,\zeta}(\pi\left(q\right))} \int_{\pi(q)}^{\infty} W\, f_{\delta,\zeta}\left(W\right) dx = \frac{1}{1-q} \int_{\pi(q)}^{\infty} x \phi_{\delta,\zeta}(w) dx. \tag{14}$$

Thus, the quantity TVaRq(W) is an average of all VAR values above at the confidence level q, which provides more information about the tail of the WXGa distribution. Further, it can also be expressed as

$$\text{TVAR}(W; q) = \text{VAR}(W; q) + e\left(\text{VAR}(W; q)\right),$$

where $e\left(\text{VAR}(W; q)\right)$ is the mean excess loss function evaluated at the $100q\%$th quantile. So, TVAR$(W; q)$ is larger than its corresponding VAR$(W; q)$ by the amount of average excess of all losses that exceed the EL$(W; q)$ value of VAR$(W; q)$. The VAR$(W; q)$ has been independently developed and is also known as the conditional tail expectation in the insurance literature ([54]). According to [52] and [6], it has also been referred to as the expected shortfall (ES) or the tail conditional expectation (TCE).

3.3. TV risk indicator

The TV risk indicator, introduced by [16], is a critical tool for assessing the variability of potential losses within the tail of a distribution. Unlike other risk metrics that focus on the central tendency or expected value of losses, the TV risk indicator specifically measures the deviation of losses from the average within the tail region of the distribution. This focus on tail variability is particularly important in risk management because it helps to capture the extent of extreme outcomes, which can have a significant impact on financial stability. The tail of a distribution represents the part where extreme values, those that are rare but potentially catastrophic, occur. The TV risk indicator quantifies how spread out these extreme losses are from their average value. A higher TV indicates greater variability and a wider range of potential outcomes within the tail, signaling that the risk of large, unpredictable losses is substantial. Conversely, a lower TV suggests that the extreme losses are more concentrated around their average, implying a more predictable risk profile within the tail. [16] not only introduced the concept of the TV risk indicator but also provided explicit formulas for calculating it under specific conditions. One of their key contributions was the development of formulas for the TV risk indicator in the context of the multivariate normal distribution. The multivariate normal distribution is a fundamental model in statistics that describes the behavior of multiple interrelated variables, each following a normal distribution with some correlation structure between them. The explicit formulas for the TV risk indicator under the multivariate normal distribution allow for precise computation of tail variance in scenarios where multiple risk factors are at play, each influencing the overall risk profile. This is particularly valuable in fields such as finance, insurance, and actuarial science, where risk exposure often depends on the interaction between various market variables, such as interest rates, stock prices, and exchange rates. By using these formulas, actuaries and risk managers can accurately measure the dispersion of extreme losses in complex, multi-variable environments. This measurement is crucial for understanding the potential impact of rare but severe events, enabling better risk mitigation strategies and more informed decision-making.

Definition 3: Let W denote a *LRV*. *The TV risk indicator (TVq(W)) can be expressed as*

$$\mathrm{TV}(W;q) = \mathbb{E}\left(W^2 | W > \pi\left(q\right)\right) - \left[\mathrm{TVAR}(W;q)\right]^2, \tag{15}$$

see [50] for more details.

3.4. TMV risk indicator

As a metric for the best portfolio choice, [31] developed the TMV risk indicator, which is based on the TCE risk indicator and the TV risk indicator.

Definition 4: Let W denote a *LRV*. *The TMV risk indicator can then be expressed as*

$$\mathrm{TMV}(W;q) = \mathrm{TVAR}(W;q) + \pi \mathrm{TV}(W;q)|_{0<\pi<1}. \tag{16}$$

Then, for any LRV, $\mathrm{TMV}(W;q) > \mathrm{TV}(W;q)$ and, for $\pi = 1$, $\mathrm{TMV}(W;q) = \mathrm{TVARq}(W;q)$.

4. Estimation

In this Section, some classical estimation methods such as the the maximum likelihood (ML) method, weighted least square (WLS) method, Anderson Darling (AD) method and Cramer–von–Mises (CVM) method are considered. We obtain the maximum likelihood estimates (MLEs) of the parameters of the WXGa distribution with complete samples . Let $w_1, \ldots, w_m$ denote the observed value of random sample of size m from the WXGa(δ, ζ) distribution. The log-likelihood function for the vector of parameters $\Theta = (\delta, \zeta)^T$ can be written as

$$l(\Theta) = \sum_{l=1}^{m} \log\left\{g(w_l;\delta)\left[2 - G(w_l,\zeta)\right] + g(w_l;\zeta)G(w_l,\delta)\right\} - 2\sum_{l=1}^{m}\log\left[2 - G(w_l,\zeta)\right].$$

The log-likelihood can be maximized either directly by using the SAS (Procedure NLMixed) or by solving the nonlinear likelihood equations obtained by differentiating (13). The components of the score vector $U()$ are given by

$$U_\delta() = \sum_{l=1}^{m} \frac{g^{(\delta)}(w_l;\delta)\,[2-G(w_l,\zeta)] + g(w_l;\zeta)G^{(\delta)}(w_l,\delta)}{g(w_l;\delta)\,[2-G(w_l,\zeta)] + g(w_l;\zeta)G(w_l,\delta)} = 0,$$
$$U_\zeta() = \sum_{l=1}^{m} \frac{-g(w_l;\zeta)G^{(b)}(w_l,\zeta) + g^{(\zeta)}(w_l;\zeta)G^{(\delta)}(w_l,\delta)}{g(w_l;\delta)\,[2-G(w_l,\zeta)] + g(w_l;\zeta)G(w_l,\delta)} + 2\sum_{i=1}^{n} \frac{G(w_l,\zeta)^{(\zeta)}}{2-G(w_l,\zeta)}. \tag{17}$$

where

$$G^{(\delta)}(w_l;\delta) = \frac{\partial G(w_l;\delta)}{\partial\delta} = \frac{w_l\, e^{-\delta\, w_l}(\delta^2+2\delta+\delta^2\, w_l - 0.5\,\delta^2\, w_l^2 - 0.5\,\delta^3\, w_l^2)}{(1+\delta)^2},$$
$$G^{(\zeta)}(w_l;\zeta) = \frac{\partial G(w_l;\zeta)}{\partial\zeta} = \frac{w_l\, e^{-\zeta\, w_l}(\zeta^2+2\gamma+\zeta^2\, w_l - 0.5\,\zeta^2\, w_l^2 - 0.5\,\zeta^3\, w_l^2)}{(1+\zeta)^2},$$
$$g^{(\delta)}(w_l;\delta) = \frac{\partial g(w_l;\delta)}{\partial\delta} = \frac{a}{1+\delta}e^{-\delta\, w_l}\left[\frac{2\delta}{1+\delta}(1+0.5\,\delta\, w_l^2) + 0.5\delta\, w_l^2 - a\, w_l(1+0.5\,\delta\, w_l^2)\right],$$
$$g^{(\zeta)}(w_l;\zeta) = \frac{\partial g(w_l;\zeta)}{\partial\zeta} = \frac{\zeta}{1+\zeta}e^{-\zeta\, w_l}\left[\frac{2\gamma}{1+\zeta}(1+0.5\,\zeta\, w_l^2) + 0.5\gamma\, w_l^2 - \zeta\, w_l(1+0.5\,\zeta\, w_l^2)\right], \tag{18}$$

We can find the root of these equations with numerical methods by R software. The weighted Least Squares estimators (WLSE) was introduced by [51]. The WLSE's are obtained by minimizing the following functions:

$$WLSE(\delta,\zeta) = \sum_{r=1}^{m} \frac{(m+1)^2(m+2)}{r(m-r+1)}\left(\frac{1-(1+\frac{\delta\, t_{r:m}}{1+\delta}+\frac{0.5\,\delta^2\, t_{r:m}^2}{1+\delta})e^{-\delta\, t_{r:m}}}{1+(1+\frac{\zeta\, t_{r:m}}{1+\zeta}+\frac{0.5\,\zeta^2\, t_{r:m}^2}{1+\zeta})e^{-\zeta\, t_{r:m}}} - \frac{r}{m+1}\right)^2.$$

Cramér–von–Mises estimator (CME) is introduced by [10]. The CMEs is obtained by minimizing the following function:

$$CME(\delta,\zeta) = \frac{1}{12m} + \sum_{r=1}^{m}\left[\frac{1-\left(1+\frac{\delta\, t_{r:m}}{1+\delta}+\frac{0.5\,\delta^2\, t_{r:m}^2}{1+\delta}\right)e^{-\delta\, t_{r:m}}}{1+\left(1+\frac{\zeta\, t_{r:m}}{1+\zeta}+\frac{0.5\,\zeta^2\, t_{r:m}^2}{1+\zeta}\right)\mathrm{e}^{-\zeta\, \mathrm{t_{r:m}}}} - \frac{2r-1}{2m}\right]^2.$$

The Anderson Darling estimator (ADE) was introduced by [5]. The ADE's are obtained by minimizing the following functions:

$$ADE(\delta,\zeta) = -m - \frac{1}{m}\sum_{r=1}^{m}(2r-1)\log\left[\frac{1-\left(1+\frac{\delta\, t_{r:m}}{1+\delta}+\frac{0.5\,\delta^2\, t_{r:m}^2}{1+\delta}\right)e^{-\delta\, t_{r:m}}}{1+\left(1+\frac{\zeta\, t_{r:m}}{1+\zeta}+\frac{0.5\,\zeta^2\, t_{r:m}^2}{1+\zeta}\right)e^{-\zeta\, t_{r:m}}}\right]$$
$$-\frac{1}{m}\sum_{r=1}^{m}(2r-1)\log\left[1-\frac{1-\left(1+\frac{\delta\, t_{m+1-r:m}}{1+\delta}+\frac{0.5\,\delta^2\, t_{m+1-r:m}^2}{1+\delta}\right)e^{-\delta\, t_{m+1-r:m}}}{1+\left(1+\frac{\zeta\, t_{m+1-r:m}}{1+\zeta}+\frac{0.5\,\zeta^2\, t_{m+1-r:m}^2}{1+\zeta}\right)e^{-\zeta\, t_{m+1-r:m}}}\right].$$

5. Simulation study

The performance of the estimated parameters are studied in this part.

For $\Theta = (\delta,\zeta) = (0.25, 0.35), (0.3, 0.45), (0.4, 0.4), (1.5, 2)$, we performed simulation analysis based on the following steps.

1. Generate M=1000 samples of the size $m = 30, 80, \ldots, 480$ from (3) .
2. Compute the estimates for the M=10000 samples, say $\left(\hat{\delta}_l, \zeta_l\right)$ for $l = 1, 2, ..., 1000$.
3. Compute the bias and mean squared errors with following equation.

$$Bias(\hat{\delta}) = \frac{1}{1000}\sum_{m=1}^{1000}(\hat{\delta}_m - \delta),\ Bias(\zeta) = \frac{1}{1000}\sum_{m=1}^{1000}(\zeta_m - \zeta),$$
$$MSE(\hat{\delta}) = \frac{1}{1000}\sum_{m=1}^{1000}(\hat{\delta}_m - \delta)^2,\ MSE(\zeta) = \frac{1}{1000}\sum_{m=1}^{1000}(\zeta_m - \zeta)^2.$$

The estimated Bias and MSE are reported in tables 1-8. For estimating parameter δ, for all method of estimation, biases are mostly negative and the absolute value of biases are approch to zero by increasing the sample size. For estimating parameter ζ, for all method of estimation, biases are mostly positive and are approch to zero by increasing the sample size. MSE for both parameters in each method are approch to zero by increasing the sample size.

Table 1. Estimated Biases for $(\delta, \gamma) = (0.25, 0.35)$

n	$WLSE(\hat{\delta})$	$CME(\hat{\delta})$	$MLE(\hat{\delta})$	$AD(\hat{\delta})$	$WLSE(\hat{\gamma})$	$CME(\hat{\gamma})$	$MLE(\hat{\gamma})$	$AD(\hat{\gamma})$
30	-0.00326	-0.014116	0.00991	-0.00661	-.00125	0 .01122	0.00820	0.00081
80	-0.01130	-0.015714	0.00678	-0.01226	0.00722	0.01438	0.00240	0.00648
130	-0.01544	-0.018587	0.00760	-0.01640	0.01023	0.01551	0.00152	0.01231
180	-0.01520	-0.018948	0.00967	-0.01598	0.01029	0.01659	0.00112	0.01170
230	-0.01410	-0.016637	0.00708	-0.01480	0.00753	0.01319	0.00104	0.00953
280	-0.01064	-0.013345	0.00196	-0.01111	0.00362	0.00910	0.00090	0.00409
330	-0.01117	-0.013613	0.00388	-0.01173	0.00671	0.01177	0.00080	0.00810
380	-0.01122	-0.013187	0.00261	-0.01175	0.00607	0.00954	0.00068	0.00738
430	-0.01226	-0.013644	0.00394	-0.01252	0.00753	0.01001	0.00064	0.00829
480	-0.01019	-0.011877	0.00032	-0.01058	0.00249	0.00558	0.00051	0.00356

Table 2. Estimated MSE for $(\delta, \gamma) = (0.25, 0.35)$

n	$WLSE(\hat{\delta})$	$CME(\hat{\delta})$	$MLE(\hat{\delta})$	$AD(\hat{\delta})$	$WLSE(\hat{\gamma})$	$CME(\hat{\gamma})$	$MLE(\hat{\gamma})$	$AD(\hat{\gamma})$
30	0.00677	0.006218	0 .00820	0.00646	0.01131	0.01169	0.01418	0.00875
80	0.00319	0.003508	0.00240	0.00317	0.00835	0.00902	0.00806	0.00677
130	0.00207	0.002321	0.00152	0.00212	0.00560	0.00640	0.00479	0.00560
180	0.00147	0.001710	0.00112	0.00152	0.00425	0.00526	0.00435	0.00421
230	0.00131	0.001518	0.00104	0.00136	0.00321	0.00450	0.00324	0.00351
280	0.00112	0.001340	0.00090	0.00115	0.00279	0.00380	0.00229	0.00257
330	0.00102	0.001206	0.00080	0.00106	0.00248	0.00346	0.00191	0.00264
380	0.00090	0.001037	0.00068	0.00093	0.00235	0.00308	0.00167	0.00252
430	0.00083	0.000951	0.00064	0.00086	0.00235	0.00303	0.00163	0.00247
480	0.00068	0.000815	0.00051	0.00071	0.00160	0.00215	0.00120	0.00174

6. Application

In this section, we introduce and analyze four real-life data applications by comparing the performance of the proposed WXGa model with several well-established models. First, we examine the four real data sets. Analyzing real-life data can be approached through numerical methods, visual techniques, or a combination of both. To assess

Table 3. Estimated Biases for $(\delta, \gamma) = (0.3, 0.45)$

n	$WLSE(\hat{\delta})$	$CME(\hat{\delta})$	$MLE(\hat{\delta})$	$AD(\hat{\delta})$	$WLSE(\hat{\gamma})$	$CME(\hat{\gamma})$	$MLE(\hat{\gamma})$	$AD(\hat{\gamma})$
30	0.00605	-0.005465	0.01018	0.00140	0.00448	0.02302	0.03486	0.01008
80	-0.01613	-0.020787	-0.00992	-0.01721	0.01866	0.02342	0.02190	0.01828
130	-0.01310	-0.018210	-0.00626	-0.01434	0.01302	0.02281	0.00988	0.01542
180	-0.01304	-0.016813	-0.00728	-0.01422	0.00357	0.01123	0.00068	0.00610
230	-0.01336	-0.018503	-0.00880	-0.01455	0.00430	0.01553	0.00359	0.00732
280	-0.01564	-0.019477	-0.01051	-0.01657	0.01063	0.02049	0.00727	0.01311
330	-0.01431	-0.018015	-0.00944	-0.01534	0.00921	0.01795	0.00487	0.01186
380	-0.00982	-0.012689	-0.00523	-0.01051	0.00215	0.00841	-0.00168	0.00385
430	-0.01134	-0.013806	-0.00621	-0.01180	0.00540	0.01004	-0.00050	0.00633
480	-0.00811	-0.010897	-0.00418	-0.00890	-0.00070	0.00498	-0.00346	0.00124

Table 4. Estimated MSE for $(\delta, \gamma) = (0.3, 0.45)$

n	$WLSE(\hat{\delta})$	$CME(\hat{\delta})$	$MLE(\hat{\delta})$	$AD(\hat{\delta})$	$WLSE(\hat{\gamma})$	$CME(\hat{\gamma})$	$MLE(\hat{\gamma})$	$AD(\hat{\gamma})$
30	0.01152	0.010925	0 .01149	0.01084	0.02260	0.02493	0.04577	0.01983
80	0.00409	0.004316	0.00302	0.00403	0.01478	0.01404	0.02060	0.01260
130	0.00272	0.003015	0.00200	0.00275	0.01041	0.01209	0.01069	0.01026
180	0.00195	0.002292	0.00149	0.00201	0.00652	0.00806	0.00575	0.00661
230	0.00162	0.002008	0.00126	0.00169	0.00511	0.00710	0.00474	0.00549
280	0.00148	0.001828	0.00109	0.00154	0.00504	0.00729	0.00513	0.00533
330	0.00136	0.001676	0.00105	0.00143	0.00417	0.00591	0.00335	0.00447
380	0.00120	0.001447	0.00095	0.00124	0.00369	0.00467	0.00328	0.00388
430	0.00103	0.001236	0.00077	0.00106	0.00340	0.00411	0.00242	0.00338
480	0.00099	0.001211	0.00077	0.00104	0.00285	0.00383	0.00249	0.00307

Table 5. Estimated for $(\delta, \gamma) = (0.4, 0.4)$

n	$WLSE(\hat{\delta})$	$CME(\hat{\delta})$	$MLE(\hat{\delta})$	$AD(\hat{\delta})$	$WLSE(\hat{\gamma})$	$CME(\hat{\gamma})$	$MLE(\hat{\gamma})$	$AD(\hat{\gamma})$
30	-0.03148	-0.050046	-0.02529	-0.03801	0.05231	0.07771	0.06197	0.05628
80	-0.03018	-0.037133	-0.02736	-0.03146	0.02005	0.02848	0.01785	0.02205
130	-0.02321	-0.026867	-0.02384	-0.02334	0.01403	0.02001	0.01264	0.01265
180	-0.02502	-0.026762	-0.02688	-0.02534	0.01234	0.01325	0.01508	0.01328
230	-0.02313	-0.024900	-0.02415	-0.02310	0.00478	0.00930	0.00668	0.00432
280	-0.01980	-0.021653	-0.02285	-0.02041	0.00212	0.00559	0.00871	0.00434
330	-0.02143	-0.022297	-0.02299	-0.02128	0.00453	0.00605	0.00771	0.00468
380	-0.01980	-0.020234	-0.02128	-0.01990	0.00115	0.00146	0.00353	0.00154
430	-0.01694	-0.018054	-0.01833	-0.01687	-0.00091	0.00032	0.00222	-0.00086
480	-0.01587	-0.015987	-0.01737	-0.01580	-0.00099	-0.00054	0.00182	-0.00092

Table 6. Estimated for $(\delta, \gamma) = (0.4, 0.4)$

n	$WLSE(\hat{\delta})$	$CME(\hat{\delta})$	$MLE(\hat{\delta})$	$AD(\hat{\delta})$	$WLSE(\hat{\gamma})$	$CME(\hat{\gamma})$	$MLE(\hat{\gamma})$	$AD(\hat{\gamma})$
30	0.02294	0.020996	0.04526	0.02205	0.03329	0.03847	0.03722	0.02714
80	0.00830	0.008957	0.00967	0.00864	0.01426	0.01495	0.00948	0.01321
130	0.00577	0.006227	0.00510	0.00575	0.01067	0.01201	0.00643	0.00850
180	0.00456	0.004758	0.00429	0.00461	0.00663	0.00606	0.00508	0.00672
230	0.00355	0.003828	0.00333	0.00350	0.00390	0.00600	0.00323	0.00344
280	0.00256	0.002868	0.00271	0.00267	0.00239	0.00369	0.00317	0.00333
330	0.00256	0.002679	0.00259	0.00257	0.00329	0.00388	0.00331	0.00334
380	0.00205	0.002103	0.00200	0.00207	0.00161	0.00162	0.00151	0.00165
430	0.00161	0.001762	0.00160	0.00161	0.00105	0.00136	0.00127	0.00106
480	0.00153	0.001628	0.00155	0.00153	0.00131	0.00153	0.00141	0.00132

how well theoretical distributions such as normal, uniform, exponential, logistic, beta, lognormal, and Weibull fit the data, we use a range of graphical tools. These include the skewness-kurtosis plot (also known as the Cullen

Table 7. Estimated for $(\delta, \gamma) = (1.5, 2)$

n	$WLSE(\hat{\delta})$	$CME(\hat{\delta})$	$MLE(\hat{\delta})$	$AD(\hat{\delta})$	$WLSE(\hat{\gamma})$	$CME(\hat{\gamma})$	$MLE(\hat{\gamma})$	$AD(\hat{\gamma})$
30	0.00002	-0.005331	0.00155	-0.00702	-0.00322	-0.01190	0.02527	0.06443
80	-0.00099	-0.003341	0.00440	-0.00279	-0.00638	-0.00813	-0.00213	0.00170
130	-0.00243	-0.005064	0.00012	-0.00374	-0.00930	-0.00616	-0.00447	-0.00606
180	-0.00221	-0.004998	0.00025	-0.00348	-0.01488	-0.00878	-0.01022	-0.01112
230	-0.00186	-0.004462	0.00076	-0.00304	-0.01037	-0.00472	-0.01080	-0.00630
280	-0.00187	-0.003972	0.00064	-0.00279	-0.01280	-0.00958	-0.01321	-0.01035
330	-0.00291	-0.004881	-0.00072	-0.00388	-0.00738	-0.00366	-0.00905	-0.00448
380	-0.00358	-0.005575	-0.00113	-0.00425	-0.00768	-0.00289	-0.01079	-0.00589
430	-0.00151	-0.003060	-0.00021	-0.00214	-0.01135	-0.00770	-0.01177	-0.00950
480	-0.00227	-0.003793	-0.00124	-0.00328	-0.00953	-0.00594	-0.00935	-0.00598

Table 8. Estimated for $(\delta, \gamma) = (1.5, 2)$

n	$WLSE(\hat{\delta})$	$CME(\hat{\delta})$	$MLE(\hat{\delta})$	$AD(\hat{\delta})$	$WLSE(\hat{\gamma})$	$CME(\hat{\gamma})$	$MLE(\hat{\gamma})$	$AD(\hat{\gamma})$
30	0.00371	0.003190	0.00245	0.00312	0.04049	0.01562	0.04766	1.12855
80	0.00171	0.001687	0.00144	0.00164	0.01498	0.01172	0.02166	0.02400
130	0.00105	0.001059	0.00087	0.00102	0.00902	0.00820	0.01006	0.00901
180	0.00083	0.000890	0.00071	0.00083	0.00623	0.00628	0.00786	0.00628
230	0.00067	0.000712	0.00056	0.00067	0.00516	0.00521	0.00465	0.00548
280	0.00058	0.000612	0.00048	0.00058	0.00457	0.00423	0.00451	0.00451
330	0.00051	0.000543	0.00040	0.00050	0.00455	0.00449	0.00406	0.00469
380	0.00043	0.000510	0.00035	0.00044	0.00365	0.00377	0.00273	0.00355
430	0.00044	0.000493	0.00037	0.00044	0.00350	0.00366	0.00298	0.00358
480	0.00039	0.000437	0.00031	0.00039	0.00317	0.00331	0.00269	0.00347

and Frey plot), which helps visualize how distributions compare in terms of their skewness and kurtosis. For improved accuracy, we also use plotting and bootstrapping techniques. While Cullen and Frey's plot provides a reasonable overview, it is limited to comparing distributions based on squared skewness and kurtosis alone. To address this limitation, we employ additional graphical methods. The "nonparametric Kernel density estimation (NKDE)" approach is used to explore the initial shape of the insurance claims density. The "Quantile-Quantile (Q-Q)" plot is employed to assess the normality of the data. The "Total Time in Test (TTT)" plot helps investigate the initial shape of the empirical hazard rate function (HRF). Finally, the "box plot" is utilized to identify extreme values, such as significant flood peaks. These diverse graphical techniques provide a comprehensive analysis of the data and the fit of the WXGa model compared to other distributions.

For all examples, the criteria of the Cramér–von Mises (W^*), the criteria of the Anderson-Darling (A^*) , akaike Information Criterion (AIC) and bayesian information criterion (BIC) are choosed. The MLE method was employed to estimate the parameters of the various distributions under consideration. We compared the performance of several distributions using MLE, including the Weibull distribution (W), the Lindley distribution (Li) introduced by [17], the generalized Lindley (GL) distribution, the power Lindley (PL) distribution proposed by [18], the generalized exponential (GE) model from [20], the XGamma distribution, and the exponentiated XGamma (Exp-XGa) distribution. These distributions were evaluated using four different real-life data sets:

The first data set consists of survival times (measured in months) for 48 patients who were treated with alkylating agents for multiple myeloma. This data was sourced from [19], providing insights into the efficacy and outcomes of the treatment. The second data set records the times between failures of secondary reactor pumps. The third data set details the exceedances of flood peaks (in cubic meters per second, m^3/s) from the Weaton River. This data was analyzed by [12] and is valuable for assessing flood risk and managing water resources. The fourth data set includes the failure times of 20 components, as reported by [42]. This data provides information on the longevity and durability of various components, essential for reliability engineering. By comparing these distributions across the diverse data sets, we aim to evaluate their performance and suitability for different types of data and applications.

This comparison helps in determining which distribution best fits the data and provides the most accurate and reliable parameter estimates.

Figure 3 gives the TTT plots for the four data sets, Figure 4 gives the box plots for the four data sets, Figure 5 gives the Q-Q plots for the four data sets, Figure 6 gives the NKDE plots for the four data sets and finally, Figure 7 gives the Cullen and Frey plot for the four data sets. Based on Figure 3, the emperical HRFs are "upside-down-bathtub", "bathtub", "bathtub" and "upside-down-bathtub"
respectively. Based on Figure 4, all real data sets have some extreme observations except the fourth dataset, and same results can be conducted from Figure 5. Due to Figure 6 the four real data sets are asymmetric bimodal and right skewed.

Second, we obtained the MLE estimators for each data using R software. The estimated parameters, standard errors and other information criteria are reported in tables 9, 10, 11 and 12. For all data sets, WXGa provide a better fit than other models. Figure 7, Figure 8, Figure 9 and Figure 10 show the estimated PDF with histogram and estimated hazard rate function. It is clearly that the new WXGa is a good selection for modelling bathtub and upside down bathtub hazard rate data sets.

Table 9. Result for survival data

model	estimatted parameters (se)		W^*	A^*	AIC	BIC
WXGa (δ, γ)	0.283	0.079	**0.038**	**0.275**	**404.89**	**408.64**
	(0.041)	(0.010)				
XGa (δ)	0.11		0.177	1.046	428.92	430.80
	(0.009)					
Li (δ)	0.078		0.094	0.566	416.29	418.16
	(0.008)					
expXGa (δ, γ)	0.079	0.506	0.208	1.214	415.30	419.04
	(0.011)	(0.092)				
GL (δ, γ)	0.057	0.568	0.101	0.606	408.67	412.42
	(0.009)	(0.108)				
PL (δ, γ)	0.184	0.747	0.069	0.431	407.13	410.88
	(0.046)	(0.070)				
Ga (δ, γ)	1.044	23.404	0.074	0.450	406.76	410.51
	(0.188)	(5.369)				
W (δ, γ)	0.039	1.006	0.074	0.452	406.82	410.56
	(0.017)	(0.111)				
GE (δ, γ)	0.042	1.053	0.073	0.447	406.75	410.49
	(0.007)	(0.202)				

7. Risk analysis and application under the exceedances of flood peaks

Risk aversion is the tendency of people to favour outcomes with low uncertainty over those with high uncertainty, even when the average outcome of the latter is equal to or higher in monetary worth than the more definite event. This tendency is shown in both economics and finance. However, no matter how a person tries to avoid risk, risk is an integral part of natural phenomena and activities. For the exceedances of flood peaks data, we propose an application for risk analysis using VAR, TVAR, TV, and TMV metrics.The risk analysis is done for some confidence levels ($q = (70\%, 75\%, 82\%, 85\%, 90\%, 95\%, 99\%, 99.95\%$ and $99.99\%)$). The four measures are estimated for the WXGa and XGa models. The XGa model is the baseline model for this application. In this paper we employ the

Table 10. Result for reactor pumps data

model	estimatted parameters (se)		W^*	A^*	AIC	BIC
WXGa (δ,γ)	3.476 (0.972)	0.909 (0.178)	**0.036**	**0.250**	**66.12**	**68.39**
XGa (δ)	1.156 (0.171)		0.110	0.668	70.92	72.06
Li (δ)	0.957 (0.150)		0.102	0.635	72.61	73.74
expXGa (δ,γ)	0.951 (0.205)	0.677 (0.178)	0.111	0.673	70.56	72.84
GL (δ,γ)	0.725 (0.178)	0.612 (0.164)	0.108	0.662	70.97	73.24
PL (δ,γ)	1.195 (0.212)	0.725 (0.112)	0.073	0.473	69.49	71.76
Ga (δ,γ)	0.745 (0.188)	2.115 (0.739)	0.078	0.501	69.51	71.78
W (δ,γ)	0.765 (0.182)	0.807 (0.129)	0.065	0.431	69.02	71.29
GE (δ,γ)	0.515 (0.154)	0.739 (0.193)	0.080	0.511	69.56	71.83

Table 11. Result for dWeaton River data

model	estimatted parameters (se)		W^*	A^*	AIC	BIC
WXGa (δ,γ)	0.932 (0.193)	0.179 (0.015)	**0.042**	**0.259**	**503.53**	**508.09**
XGa (δ)	0.204 (0.015)		0.152	0.989	534.92	537.20
Li (δ)	0.153 (0.012)		0.139	0.852	530.42	532.70
expXGa (δ,γ)	0.147 (0.017)	0.509 (0.074)	0.147	0.967	512.55	517.10
GL (δ,γ)	0.104 (0.014)	0.508 (0.076)	0.132	0.822	509.34	513.90
PL (δ,γ)	0.338 (0.055)	0.699 (0.056)	0.150	0.866	508.44	512.99
Ga (δ,γ)	0.838 (0.121)	14.549 (2.812)	0.130	0.751	506.68	511.24
W (δ,γ)	0.109 (0.030)	0.901 (0.085)	0.137	0.785	506.99	511.55
GE (δ,γ)	0.072 (0.011)	0.828 (0.123)	0.128	0.742	506.58	511.14

WXGa model to analyze the risk however there many other usefull models with chan be used for the same aim (see [58], [34], [35], [36], [37], [38], [39], [30], [28], [14] and [45] for more details).

Table 13 reports the KRIs for the WXGa and XGa models. For the WXGa model, the quantity VAR$(W;q)$ ranges from 6.107068 to 14.99099, TVAR$(W;q)$ ranges from 10.007352 to 17.867624, TV$(W;q)$ ranges from 3.077639 to 3.398732 and TMV$(W;q)$ ranges from 14.697092 to 18.767642. For the XGa model, VAR$(W;q)$

Table 12. Result for failure time data

model	estimatted parameters (se)		W^*	A^*	AIC	BIC
WXGa (δ, γ)	0.325 (0.070)	0.068 (0.011)	**0.084**	**0.468**	**173.94**	**175.93**
XGa (δ)	0.089 (0.012)		0.192	1.120	189.47	190.47
Li (δ)	0.063 (0.009)		0.168	0.964	182.62	183.61
expXGa (δ, γ)	0.065 (0.014)	0.514 (0.143)	0.195	1.136	185.04	187.03
GL (δ, γ)	0.047 (0.012)	0.601 (0.177)	0.168	0.963	181.38	183.37
PL (δ, γ)	0.143 (0.061)	0.771 (0.114)	0.164	0.943	181.14	183.13
Ga (δ, γ)	1.141 (0.322)	26.904 (9.457)	0.162	0.927	180.75	182.74
W (δ, γ)	0.024 (0.018)	1.075 (0.188)	0.163	0.932	180.81	182.80
GE (δ, γ)	0.035 (0.010)	1.148 (0.344)	0.162	0.927	180.76	182.75

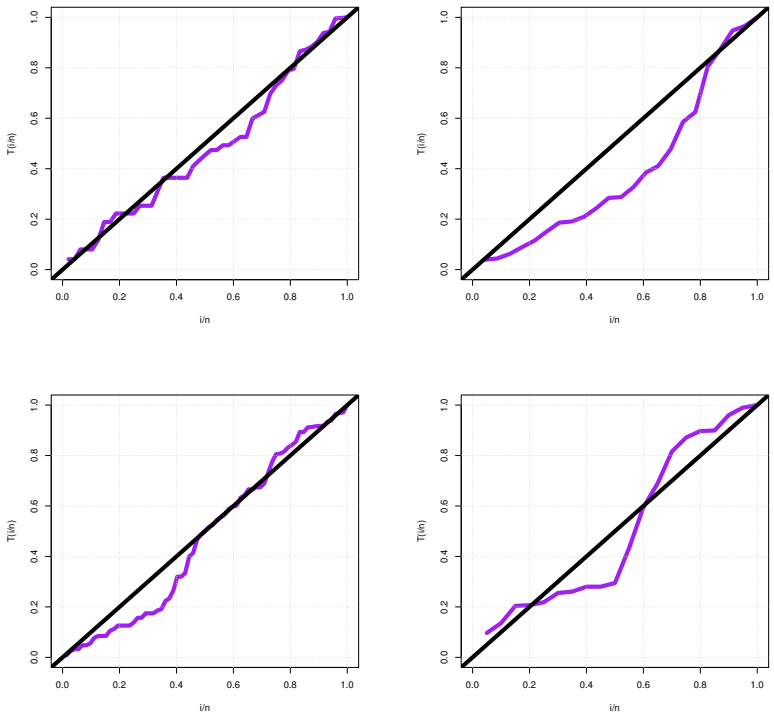

Figure 3. The TTT plots.

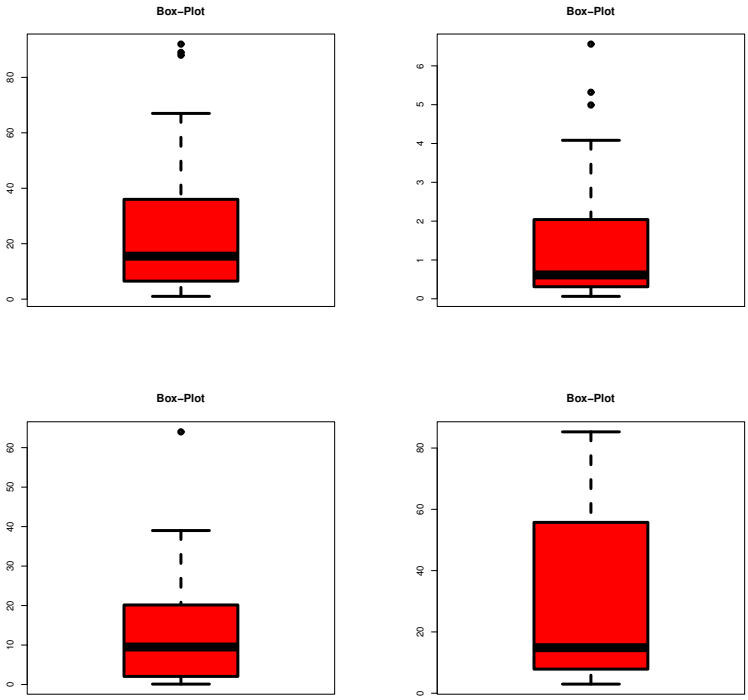

Figure 4. The box plots.

ranges from 5.004395 to 9.431434, TVAR$(W;q)$ ranges from 5.721463 to9.660566, TV$(W;q)$ ranges from 2.669988 to 2.880101, and TMV ranges from 5.861466 to 9.7665812. The conclusions follow as:

$$\text{VAR}(W;q) \text{ for WXGa} > \text{VAR}(W;q) \text{ for XGa} \forall\ q,$$

$$\text{TVAR}(W;q) \text{ for WXGa} > \text{TVAR}(W;q) \text{ for XGa} \forall\ q,$$

$$\text{TV}(W;q) \text{ for WXGa} > \text{TV}(W;q) \text{ for XGa} \forall\ q,$$

$$\text{TMV for WXGa} > \text{TMV for XGa} \forall\ q,$$

and generally

$$\text{VAR}(W;q) < \text{TVAR}(W;q) < \text{TMV}(W;q)\ \forall\ q.$$

Also, $\forall\ q$, EL$(W;q)$ is evaluated where for the WXGa model the EL$(W;q)$ decreases as q increases and it started with $3.900284|q = 70\%$ and eded with $2.876634|q = 99.99\%$. For the XGa model the EL$(W;q)$ decreases as q increases and it started with $0.717068|q = 70\%$ and eded with $0.229132|q = 99.99\%$. EL$(W;q)$ for the WXGa model>EL$(W;q)$ for the XGa model $\forall\ q$.

Figure 11 provides three scatter plots, autocorrelation function and partial autocorrelation function for the the exceedances of flood peaks data. Figure 12 reports the plots of VAR, TVAR, TV, TMV and EL. Each plot provides a graphical comparison between WXGa and XGa models. Based on Figure 12, the WXGa model has a heavier tail than the XGa distribution for all KRIs. Therefore, when measuring risk and issues of disclosure, we prefer the model with has a heavier tail. Table 13 below provides a detailed comparison of KRIs for the exceedances of flood

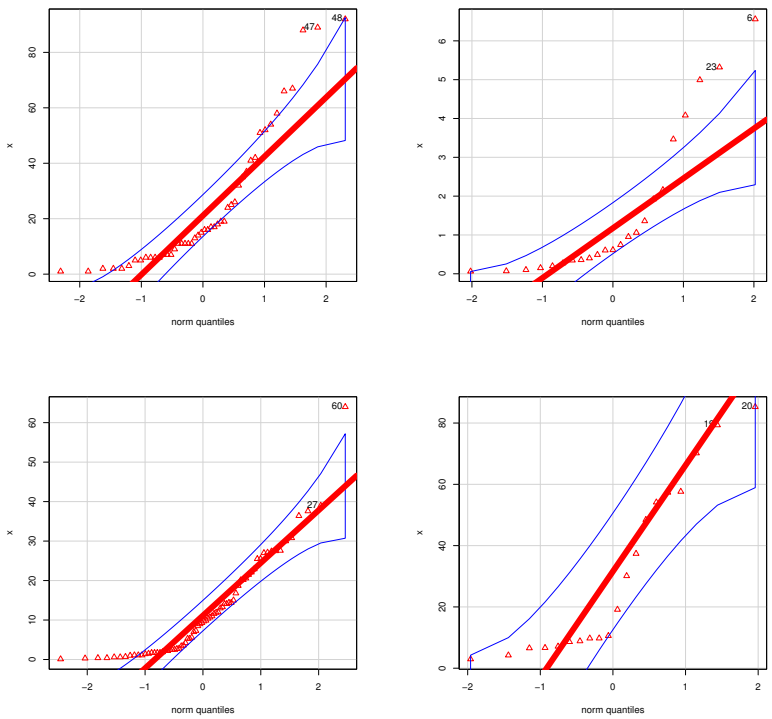

Figure 5. The Q-Q plots.

peaks data, contrasting the performance of the WXGa model with the XGa model. This comparison is conducted across a range of confidence levels from 0.70 to 0.9999. The WXGa Model: Exhibits consistently higher VAR values across all confidence levels. For instance, at the 0.70 confidence level, the WXGa model predicts a VAR of 6.107068, compared to the XGa model's 5.004395. This trend continues at higher confidence levels, with the WXGa model showing a VAR of 14.99099 at the 0.9999 confidence level, while the XGa model's VAR is 9.431434. These higher VAR values suggest that the WXGa model predicts a higher potential maximum loss, reflecting a more conservative estimate of risk exposure. Also shows higher TVAR values compared to the XGa model across all confidence levels. For example, at the 0.70 confidence level, the WXGa model's TVAR is 10.007352, while the XGa model's TVAR is 5.721463. This indicates that the WXGa model anticipates larger expected losses conditional on exceeding the VAR threshold, reinforcing the notion of greater risk exposure in extreme scenarios. Generally presents higher or comparable TV values than the XGa model. For instance, the WXGa model has a TV of 3.077639 at the 0.70 confidence level, compared to the XGa models 2.669988. Higher tail variance values in the WXGa model suggest it accounts for greater variability in extreme losses, reflecting a more comprehensive understanding of risk distribution. Displays higher TMV values across the board. At the 0.70 confidence level, the WXGa model's TMV is 14.697092, while the XGa models TMV is 5.861466. This metric, which combines the mean and variance of losses in the tail, indicates that the WXGa model captures more risk associated with extreme events, highlighting its ability to represent severe loss scenarios more effectively.

The WXGa model shows consistently higher EL values compared to the XGa model. For example, at the 0.70 confidence level, the EL for the WXGa model is 3.900284, compared to 0.717068 for the XGa model. This suggests that the WXGa model anticipates higher average losses when extreme flood peaks are considered, reinforcing its

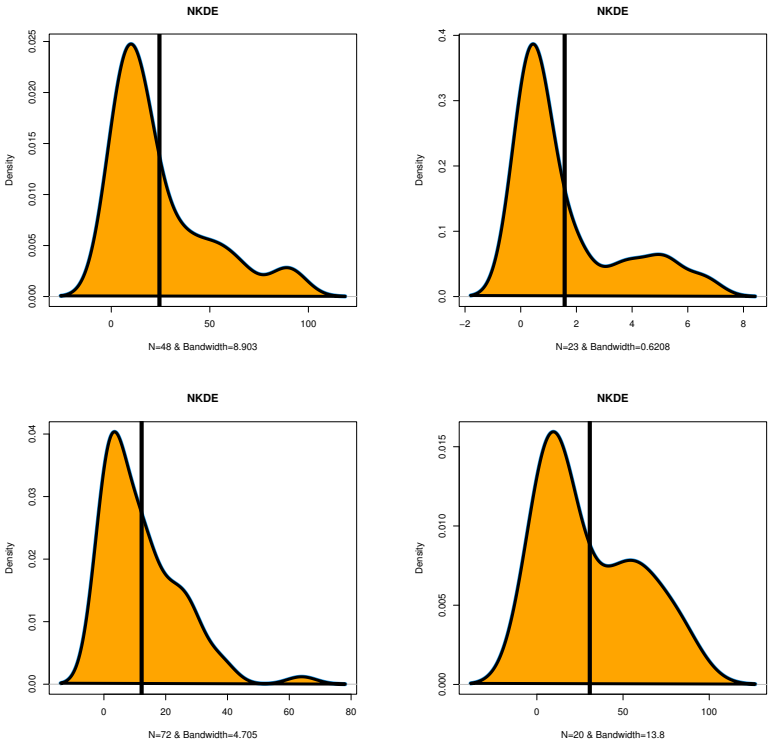

Figure 6. NKDE plots.

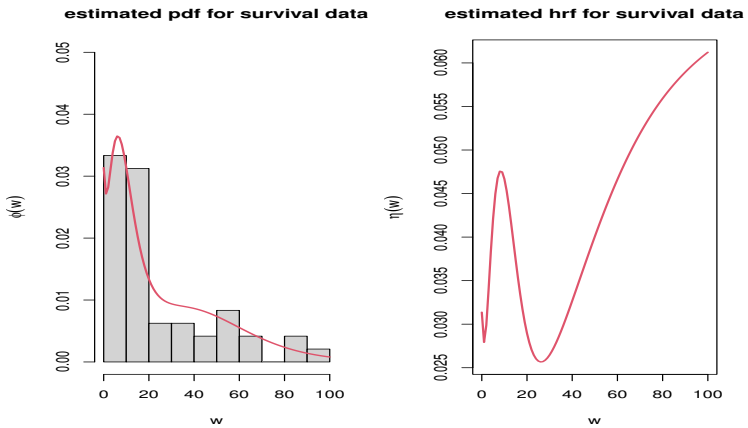

Figure 7. Estimated pdf and hrf for survival data.

role in capturing more substantial risk. The WXGa model's metrics are notably higher at more extreme confidence levels (e.g., 0.9995 and 0.9999) compared to the XGa model. This trend indicates that the WXGa model provides a more cautious and conservative estimate of risk, particularly in scenarios involving rare but severe flood events. For example, the WXGa model's VAR at 9999 is 14.99099, whereas the XGa models VAR at the same level is

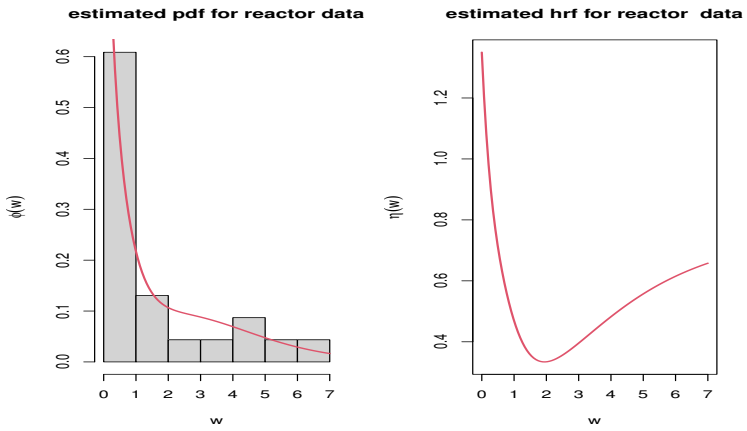

Figure 8. Estimated pdf and hrf for reactor pump data.

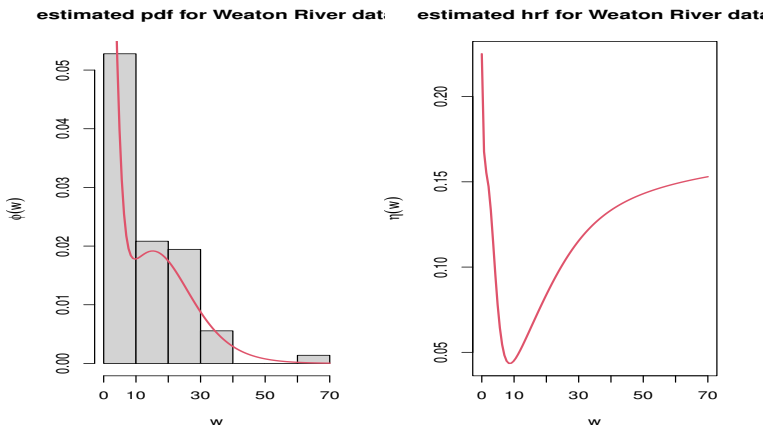

Figure 9. Estimated pdf and hrf for Weaton River data.

9.431434. The consistently higher risk estimates provided by the WXGa model suggest it offers a more conservative approach to risk assessment, particularly in the context of extreme flood peaks. This can be advantageous for risk management and financial planning, as it ensures that potential losses are accounted for more comprehensively, thus providing a buffer against severe events. The WXGa models ability to capture higher potential losses, greater variability, and more substantial average losses makes it a valuable tool for understanding and preparing for extreme risk scenarios. In fact, risk analysis is closely related to the extreme value theory, as financial or actuarial risks are often caused by unexpected financial events. The extreme value theory includes three basic distributions, but there are many important extensions that have contributed to expanding the theory. For more details and applications, see [21], [26], [9], [59], [15], [63], [40] and [4].

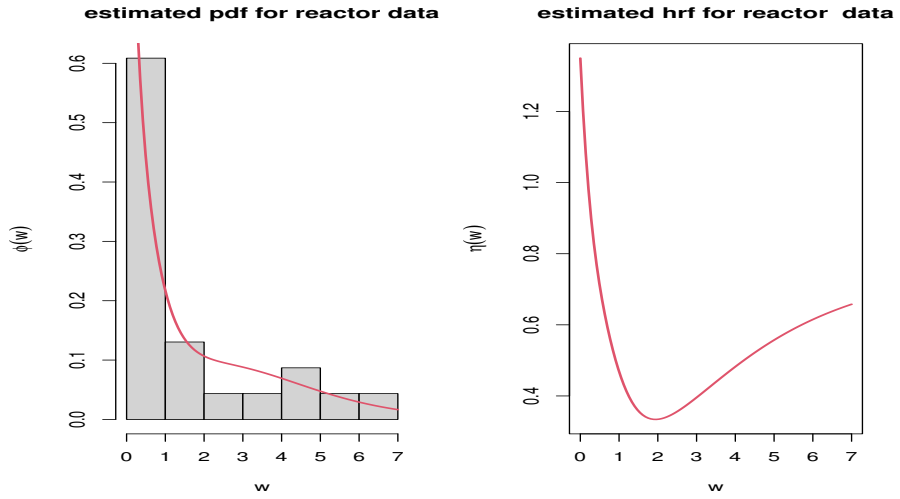

Figure 10. Estimated pdf and hrf for failure time data.

Table 13: KRIs under thethe exceedances of flood peaks data.

Model	q	VAR$(W;q)$	TVAR$(W;q)$	TV$(W;q)$	TMV$(W;q)$	EL$(W;q)$
WXGa	70%	6.107068	10.007352	3.077639	14.697092	3.900284
	75%	7.268941	11.141077	3.117321	14.997978	3.872136
	82%	8.481329	13.676029	3.170909	15.002943	5.194700
	85%	8.722445	13.984716	3.191098	15.834933	5.262271
	90%	9.078533	14.156375	3.202032	16.052160	5.077842
	95%	9.662075	15.734118	3.267672	16.742077	6.072043
	99%	10.94994	16.352006	3.333333	17.070798	5.402066
	99.95%	12.94954	17.867624	3.379876	18.046487	4.918084
	99.99%	14.99099	17.867624	3.398732	18.767642	2.876634
XGa	70%	5.004395	5.721463	2.669988	5.861466	0.717068
	75%	6.193295	6.988843	2.696512	7.449665	0.795548
	82%	7.046690	7.543656	2.729823	7.193565	0.496966
	85%	7.335459	7.998723	2.757551	8.068723	0.663264
	90%	7.494305	8.991763	2.800981	8.294463	1.497458
	95%	7.983715	9.055544	2.818734	8.790365	1.071829
	99%	8.615416	9.109447	2.838787	9.494322	0.494031
	99.95%	8.999853	9.207645	2.859864	9.3393574	0.207792
	99.99%	9.431434	9.660566	2.880101	9.7665812	0.229132

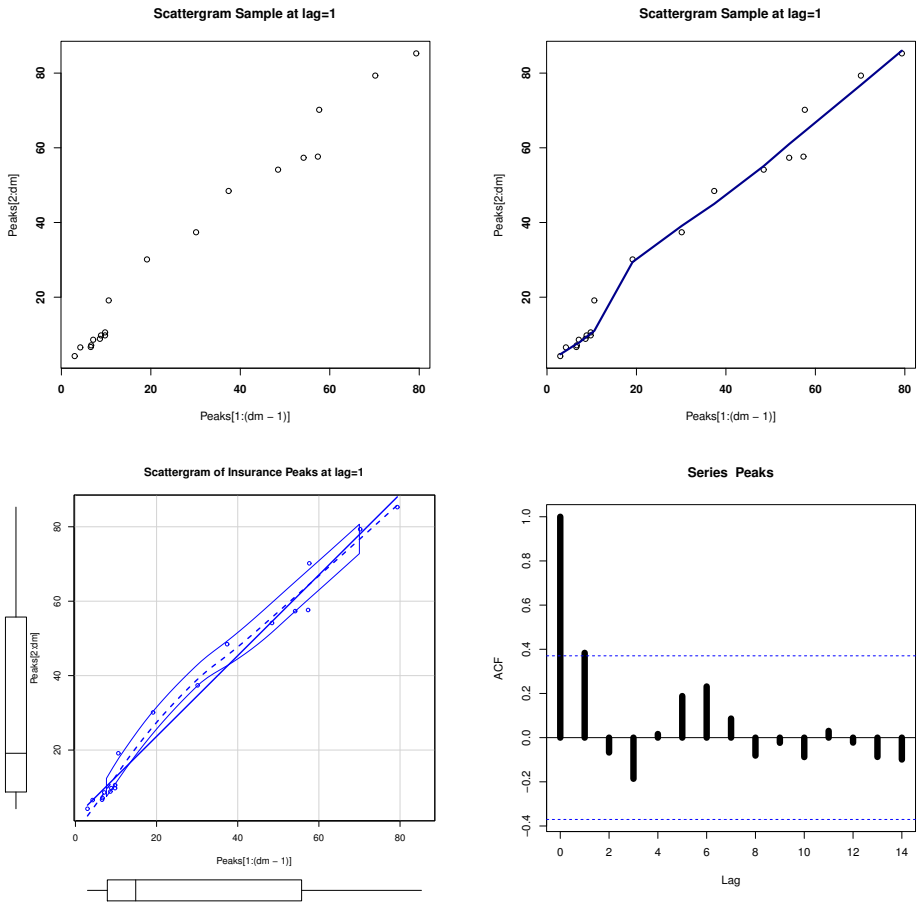

Figure 11. Scatter plots, autocorrelation function and partial autocorrelation function.

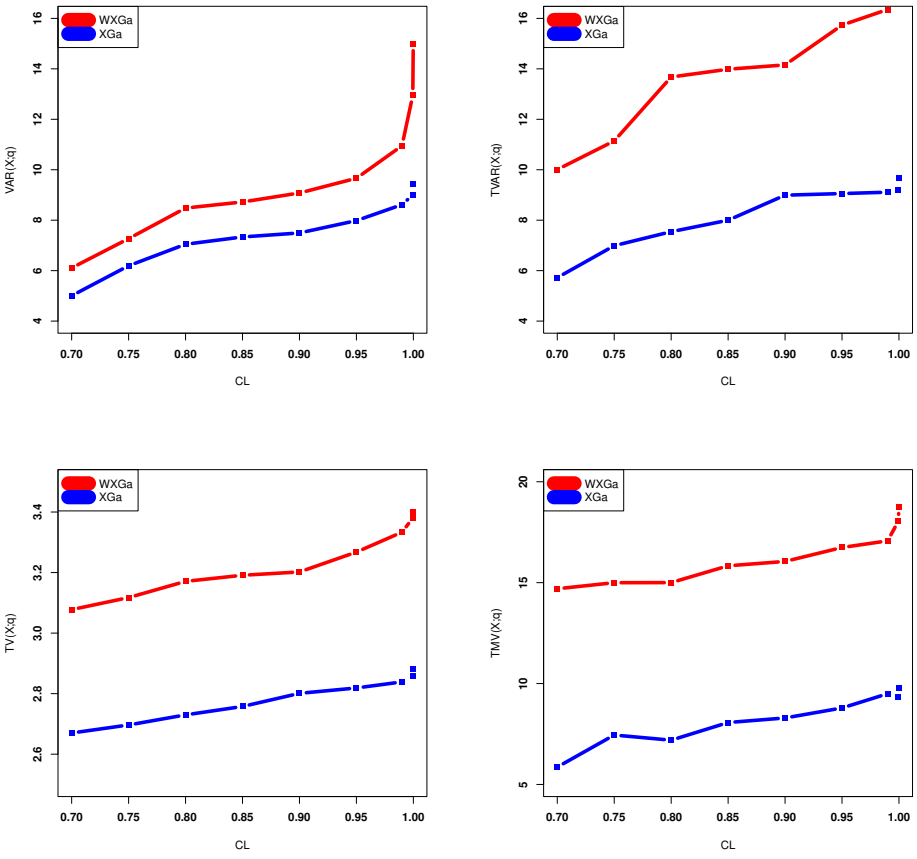

Figure 12. Plots of the VaR, TVaR, TV and TMV.

8. Concluding remarks

Continuous distributions are highly effective for characterizing risk exposure. Ideally, a single value or a small set of values is used to quantify the level of risk exposure. These values are generated by specific models and are known as key risk indicators (KRIs). To address this need, we introduce a new two-parameter lifetime distribution called the Weighted XGamma (WXGa) distribution. This new distribution offers several valuable properties, including moments, mean past lifetime, residual entropy, order statistics, as well as asymptotic and extreme value characteristics. We estimate the parameters of the WXGa distribution using various methods, including Maximum Likelihood Estimation (MLE). To ensure the reliability of these estimation methods, we analyze Bias and Mean Squared Error (MSE) plots. These plots demonstrate that as the sample size increases, both bias and MSE approach zero, confirming the validity of our estimation techniques. We assess the flexibility and effectiveness of the WXGa distribution by applying it to four real-life data sets and comparing its performance with other established distributions. The results, presented in tables and figures, show that the WXGa model consistently provides better fits than competing models. This comparison underscores the advantages of the WXGa distribution in practical applications. For risk analysis, particularly in the context of insurance claims data, we employ four essential risk indicators: Value-at-Risk (VAR), Tail Value-at-Risk (TVAR), Tail Variance (TV), and Tail Mean-Variance (TMV). These metrics are specifically developed for the WXGa model. Additionally, we present a risk analysis using these indicators to evaluate the exceedances of flood peaks, highlighting the importance and effectiveness of the WXGa model in assessing risk exposure.

REFERENCES

1. Ahmed, B., Ali, M. M. and Yousof, H. M. (2022). A Novel G Family for Single Acceptance Sampling Plan with Application in Quality and Risk Decisions, Annals of Data Science, 10.1007/s40745-022-00451-3
2. Alizadeh, M., Afshari, M., Contreras-Reyes, J. E., Mazarei, D., & Yousof, H. M. (2024). The Extended Gompertz Model: Applications, Mean of Order P Assessment and Statistical Threshold Risk Analysis Based on Extreme Stresses Data. IEEE Transactions on Reliability, doi: 10.1109/TR.2024.3425278.
3. Alizadeh, M., Afshari, M., Ranjbar, V., Merovci, F. and Yousof, H. M. (2023). A novel XGamma extension: applications and actuarial risk analysis under the reinsurance data. São Paulo Journal of Mathematical Sciences, 1-31.
4. Almazah, M.M.A., Almuqrin, M.A., Eliwa, M.S., El-Morshedy, M., Yousof, H.M. (2023). Modeling Extreme Values Utilizing an Asymmetric Probability Function. Symmetry 2021, 13, 1730. https://doi.org/10.3390/sym13091730
5. Anderson, T. W. and Darling, D. A. (1952). Asymptotic theory of certain "goodness of fit" criteria based on stochastic processes. The annals of mathematical statistics, 193-212.
6. Acerbi, C. and Tasche, D. (2002), On the coherence of expected shortfall, Journal of Banking and Finance, 26, 1487-1503.
7. Artzner, P. (1999). Application of coherent risk measures to capital requirements in insurance. N. Am. Actuar. J., 3, 11–25.
8. Bantan, R., Hassan, A. S., Elsehetry, M. and Kibria, B. M. (2020). Half-logistic XGamma distribution: Properties and estimation under censored samples. Discrete Dynamics in Nature and Society, 2020.
9. Chakraborty, S., Handique, L., Altun, E., & Yousof, H. M. (2019). A New Statistical Model for Extreme Values: Properties and Applications. Int. J. Open Problems Compt. Math, 12(1).
10. Choi, K. and Bulgren, W. (1968). An estimation procedure for mixtures of distributions. Journal of the Royal Statistical Society. Series B (Methodological), 444-460.
11. Cordeiro, G. M., Altun, E., Korkmaz, M. C., Pescim, R. R. and Afify, A. Z. and Yousof, H. M. (2020). The XGamma Family: Censored Regression Modelling and Applications. Revstat Statistical Journal, 18(5), 593–612.
12. Cordeiro, G. M., Ortega, E. M., da Cunha, D. C. (2013). The exponentiated generalized class of distributions.Journal of data science, 11(1), 1-27.
13. Elbatal, I., Diab, L. S., Ghorbal, A. B., Yousof, H. M., Elgarhy, M. and Ali, E. I. (2024). A new losses (revenues) probability model with entropy analysis, applications and case studies for value-at-risk modeling and mean of order-P analysis. AIMS Mathematics, 9(3), 7169-7211.
14. Elgohari, H. and Yousof, H. (2020). A generalization of lomax distribution with properties, copula and real data applications. Pakistan Journal of Statistics and Operation Research, 697-711.
15. Elgohari, H. and Yousof, H. M. (2021). A New Extreme Value Model with Different Copula, Statistical Properties and Applications. Pakistan Journal of Statistics and Operation Research, 17(4), 1015-1035. https://doi.org/10.18187/pjsor.v17i4.3471
16. Furman, E., Landsman, Z. (2006). Tail variance premium with applications for elliptical portfolio of risks. ASTIN Bulletin, 36 (2), 433–462
17. Ghitany, M. E., Atieh, B., Nadarajah, S. (2008). Lindley distribution and its application. Mathematics and computers in simulation, 78(4), 493-506.
18. Ghitany, M. E., Al-Mutairi, D. K., Balakrishnan, N., Al-Enezi, L. J. (2013). Power Lindley distribution and associated inference. Computational Statistics Data Analysis, 64, 20-33.

19. Gomes, M. I., Ferreira, M., Leiva, V. (2012). The extreme value Birnbaum-Saunders model, its moments and an application in biometry. Biometrical Letters, 49(2), 81-94.
20. Gupta, R. D., Kundu, D. (1999). Theory methods: Generalized exponential distributions. Australian New Zealand Journal of Statistics, 41(2), 173-188.
21. Haq, M. A. ul, Yousof, H. M., & Hashmi, S. (2017). A New Five-Parameter Fréchet Model for Extreme Values. Pakistan Journal of Statistics and Operation Research, 13(3), 617-632.
22. Hashempour, M., Alizadeh, M. and Yousof, H. M. (2023). A New Lindley Extension: Estimation, Risk Assessment and Analysis Under Bimodal Right Skewed Precipitation Data. Annals of Data Science, 1-40.
23. Hamed, M. S., Cordeiro, G. M. and Yousof, H. M. (2022). A New Compound Lomax Model: Properties, Copulas, Modeling and Risk Analysis Utilizing the Negatively Skewed Insurance Claims Data. Pakistan Journal of Statistics and Operation Research, 18(3), 601-631. https://doi.org/10.18187/pjsor.v18i3.3652
24. Hamedani, G. G., Goual, H., Emam, W., Tashkandy, Y., Ahmad Bhatti, F., Ibrahim, M. and Yousof, H. M. (2023). A new right-skewed one-parameter distribution with mathematical characterizations, distributional validation, and actuarial risk analysis, with applications. Symmetry, 15(7), 1297.
25. Ibrahim, M.; Emam, W.; Tashkandy, Y.; Ali, M.M.; Yousof, H.M. (2023). Bayesian and Non-Bayesian Risk Analysis and Assessment under Left-Skewed Insurance Data and a Novel Compound Reciprocal Rayleigh Extension. Mathematics 2023, 11, 1593. https://doi.org/10.3390/ math11071593
26. Jahanshahi, S.M.A., Yousof, H. M. and Sharma, V.K. (2019). The Burr X Fréchet Model for Extreme Values: Mathematical Properties, Classical Inference and Bayesian Analysis. Pak. J. Stat. Oper. Res., 15(3), 797-818.
27. Khedr, A. M., Nofal, Z. M., El Gebaly, Y. M. and Yousof, H. M. (2023). A Novel Family of Compound Probability Distributions: Properties, Copulas, Risk Analysis and Assessment under a Reinsurance Revenues Data Set. Thailand Statistician, forthcoming.
28. Korkmaz, M. C., Altun, E., Chesneau, C., & Yousof, H. M. (2022). On the unit-Chen distribution with associated quantile regression and applications. Mathematica Slovaca, 72(3), 765-786.
29. Korkmaz, M. Ç., Altun, E., Yousof, H. M., Afify, A. Z. and Nadarajah, S. (2018). The Burr X Pareto Distribution: Properties, Applications and VAR Estimation. Journal of Risk and Financial Management, 11(1), 1.
30. Korkmaz, M. Ç., Cordeiro, G. M., Yousof, H. M., Pescim, R. R., Afify, A. Z., & Nadarajah, S. (2019). The Weibull Marshall–Olkin family: Regression model and application to censored data. Communications in Statistics-Theory and Methods, 48(16), 4171-4194.
31. Landsman, Z. (2010). On the tail mean–variance optimal portfolio selection. Insur. Math. Econ., 46, 547–553.
32. Leadbetter, M. R., Lindgren, G., Rootzn, H. (2012). Extremes and related properties of random sequences and processes. Springer Science Business Media.
33. Loubna, H., Goual, H., Alghamdi, F. M., Mustafa, M. S., Tekle Mekiso, G., Ali, M. M., ... & Yousof, H. M. (2024). The quasi-XGamma frailty model with survival analysis under heterogeneity problem, validation testing, and risk analysis for emergency care data. Scientific Reports, 14(1), 8973.
34. Mansour, M. M., Ibrahim, M., Aidi, K., Butt, N. S., Ali, M. M., Yousof, H. M., & Hamed, M. S. (2020). A New Log-Logistic Lifetime Model with Mathematical Properties, Copula, Modified Goodness-of-Fit Test for Validation and Real Data Modeling. Mathematics, 8(9), 1508.
35. Mansour, M. M., Butt, N. S., Ansari, S. I., Yousof, H. M., Ali, M. M., & Ibrahim, M. (2020). A new exponentiated Weibull distribution's extension: copula, mathematical properties and applications. Contributions to Mathematics, 1 (2020) 57–66. DOI: 10.47443/cm.2020.0018
36. Mansour, M., Korkmaz, M. Ç., Ali, M. M., Yousof, H. M., Ansari, S. I., & Ibrahim, M. (2020). A generalization of the exponentiated Weibull model with properties, Copula and application. Eurasian Bulletin of Mathematics, 3(2), 84-102.
37. Mansour, M., Rasekhi, M., Ibrahim, M., Aidi, K., Yousof, H. M., & Elrazik, E. A. (2020). A New Parametric Life Distribution with Modified Bagdonavičius–Nikulin Goodness-of-Fit Test for Censored Validation, Properties, Applications, and Different Estimation Methods. Entropy, 22(5), 592.
38. Mansour, M., Yousof, H. M., Shehata, W. A. M., & Ibrahim, M. (2020). A new two parameter Burr XII distribution: properties, copula, different estimation methods and modeling acute bone cancer data. Journal of Nonlinear Science and Applications, 13(5), 223-238.
39. Mansour, M. M., Butt, N. S., Yousof, H. M., Ansari, S. I., & Ibrahim, M. (2020). A Generalization of Reciprocal Exponential Model: Clayton Copula, Statistical Properties and Modeling Skewed and Symmetric Real Data Sets. Pakistan Journal of Statistics and Operation Research, 16(2), 373-386.
40. Minkah, R., de Wet, T., Ghosh, A., & Yousof, H. M. (2023). Robust extreme quantile estimation for Pareto-type tails through an exponential regression model. Communications for Statistical Applications and Methods, 30(6), 531-550.
41. Mohamed, H. S., Cordeiro, G. M., Minkah, R., Yousof, H. M., & Ibrahim, M. (2024). A size-of-loss model for the negatively skewed insurance claims data: applications, risk analysis using different methods and statistical forecasting. Journal of Applied Statistics, 51(2), 348-369.
42. Murthy, D. P., Xie, M., Jiang, R. (2004). Weibull models Vol. 505. John Wiley Sons.
43. Para, B. A., Jan, T. R. and Bakouch, H. S. (2020). Poisson XGamma distribution: A discrete model for count data analysis. Model Assisted Statistics and Applications, 15(2), 139-151.
44. Ranjbar, V., Alizadeh, M., Afshari, M., & Yousof, H. M. (2024). Odd Log-Logistic XGamma Model: Bayesian and Classical Estimation with Risk Analysis Utilizing Reinsurance Revenues Data. Journal of Statistical Theory and Applications, 1-34.
45. Rasekhi, M., Altun, E., Alizadeh, M. and Yousof, H. M. (2022). The Odd Log-Logistic Weibull-G Family of Distributions with Regression and Financial Risk Models. Journal of the Operations Research Society of China, 10(1), 133-158.
46. Rasekhi, M., Saber, M. M., & Yousof, H. M. (2020). Bayesian and classical inference of reliability in multicomponent stress-strength under the generalized logistic model. Communications in Statistics-Theory and Methods, 50(21), 5114-5125.
47. Salem, M., Emam, W., Tashkandy, Y., Ibrahim, M., Ali, M. M., Goual, H. and Yousof, H. M. (2023). A new lomax extension: Properties, risk analysis, censored and complete goodness-of-fit validation testing under left-skewed insurance, reliability and medical data. Symmetry, 15(7), 1356.

48. Sen, S., Korkmaz, M. C. and Yousof, H. M. (2018). The quasi XGamma-Poisson distribution. ISTATISTIK: JOURNAL OF THE TURKISH STATISTICAL ASSOCIATION, 11(3), 65-76.
49. Sen, S., Maiti, S. S., Chandra, N. (2016). The XGamma distribution: statistical properties and application.Journal of Modern Applied Statistical Methods, 15(1), 38.
50. Shrahili, M.; Elbatal, I. and Yousof, H. M. (2021). Asymmetric Density for Risk Claim-Size Data: Prediction and Bimodal Data Applications. Symmetry 2021, 13, 2357.
51. Swain, J. J., Venkatraman, S., and Wilson, J. R. (1988). Least-squares estimation of distribution functions in johnson's translation system. Journal of Statistical Computation and Simulation, 29, 271- 297.
52. Tasche, D. (2002), Expected Shortfall and Beyond, Journal of Banking and Finance, 26, 1519-1533.
53. Teghri, S., Goual, H., Loubna, H., Butt, N. S., Khedr, A. M., Yousof, H. M., ... & Salem, M. (2024). A New Two-Parameters Lindley-Frailty Model: Censored and Uncensored Schemes under Different Baseline Models: Applications, Assessments, Censored and Uncensored Validation Testing. Pakistan Journal of Statistics and Operation Research, 109-138.
54. Wirch J. (1999), Raising Value at Risk,North American Actuarial Journal, 3, 106-115.
55. Yadav, A. S., Maiti, S. S. and Saha, M. (2021). The inverse XGamma distribution: statistical properties and different methods of estimation. Annals of Data Science, 8(2), 275-293.
56. Yadav, A. S., Saha, M., Tripathi, H., Kumar, S. (2021). The Exponentiated XGamma Distribution: a New Monotone Failure Rate Model and Its Applications to Lifetime Data. Statistica, 81(3), 303-334.
57. Yadav, A. S., Shukla, S., Goual, H., Saha, M. and Yousof, H. M. (2022). Validation of XGamma exponential model via Nikulin-Rao-Robson goodness-of- fit test under complete and censored sample with different methods of estimation. Statistics, Optimization & Information Computing, 10(2), 457-483.
58. Yousof, H. M., Afify, A. Z., Abd El Hadi, N. E., Hamedani, G. G., & Butt, N. S. (2016). On six-parameter Fréchet distribution: properties and applications. Pakistan Journal of Statistics and Operation Research, 281-299.
59. Yousof, H. M., Jahanshahi, S. M. A., Ramires, T. G., Aryal, G. R., & Hamedani, G. G. (2018). A new distribution for extreme values: regression model, characterizations and applications. Journal of Data Science, 16(4), 677 -706.
60. Yousof, H. M., Ansari, S. I., Tashkandy, Y., Emam, W., Ali, M. M., Ibrahim, M., Alkhayyat, S. L. (2023). Risk Analysis and Estimation of a Bimodal Heavy-Tailed Burr XII Model in Insurance Data: Exploring Multiple Methods and Applications. Mathematics. 2023; 11(9):2179. https://doi.org/10.3390/math11092179
61. Yousof, H.M.; Emam, W.; Tashkandy, Y.; Ali, M.M.; Minkah, R.; Ibrahim, M. (2023). A Novel Model for Quantitative Risk Assessment under Claim-Size Data with Bimodal and Symmetric Data Modeling. Mathematics 2023, 11, 1284. https://doi.org/10.3390/math11061284
62. Yousof, H. M., Saber, M. M., Al-Nefaie, A. H., Butt, N. S., Ibrahim, M. and Alkhayyat, S. L. (2024). A discrete claims-model for the inflated and over-dispersed automobile claims frequencies data: Applications and actuarial risk analysis. Pakistan Journal of Statistics and Operation Research, 261-284.
63. Yousof, H.M.; Tashkandy, Y.; Emam, W.; Ali, M.M.; Ibrahim, M. (2023). A New Reciprocal Weibull Extension for Modeling Extreme Values with Risk Analysis under Insurance Data. Mathematics 2023, 11, 966. https://doi.org/10.3390/ math11040966